Virology 458-459 (2014) 136–150

Contents lists available at ScienceDirect

Virology

journal homepage: www.elsevier.com/locate/yviro

Biogenesis of non-structural protein 1 (nsp1) and nsp1-mediated type I interferon modulation in arteriviruses

Mingyuan Han [a], Chi Yong Kim [a], Raymond R.R. Rowland [b], Ying Fang [b], Daewoo Kim [a], Dongwan Yoo [a,*]

[a] Department of Pathobiology, University of Illinois at Urbana-Champaign, 2001 South Lincoln Avenue, Urbana, IL 61802, USA
[b] Department of Diagnostic Medicine and Pathobiology, Kansas State University, Manhattan, KS 66506, USA

ARTICLE INFO

Article history:
Received 7 February 2014
Returned to author for revisions
3 March 2014
Accepted 22 April 2014
Available online 13 May 2014

Keywords:
Arteriviridae
PRRSV
EAV
LDV
SHFV
nsp1
IFN antagonism
CBP degradation

ABSTRACT

Type I interferons (IFNs-α/β) play a key role for the antiviral state of host, and the porcine arterivirus; porcine reproductive and respiratory syndrome virus (PRRSV), has been shown to down-regulate the production of IFNs during infection. Non-structural protein (nsp) 1 of PRRSV has been identified as a viral IFN antagonist, and the nsp1α subunit of nsp1 has been shown to degrade the CREB-binding protein (CBP) and to inhibit the formation of enhanceosome thus resulting in the suppression of IFN production. The study was expanded to other member viruses in the family Arteriviridae: equine arteritis virus (EAV), murine lactate dehydrogenase-elevating virus (LDV), and simian hemorrhagic fever virus (SHFV). While PRRSV–nsp1 and LDV–nsp1 were auto-cleaved to produce the nsp1α and nsp1β subunits, EAV–nsp1 remained uncleaved. SHFV–nsp1 was initially predicted to be cleaved to generate three subunits (nsp1α, nsp1β, and nsp1γ), but only two subunits were generated as SHFV–nsp1αβ and SHFV–nsp1γ. The papain-like cysteine protease (PLP) 1α motif in nsp1α remained inactive for SHFV, and only the PLP1β motif of nsp1β was functional to generate SHFV–nsp1γ subunit. All subunits of arterivirus nsp1 were localized in the both nucleus and cytoplasm, but PRRSV–nsp1β, LDV–nsp1β, EAV–nsp1, and SHFV–nsp1γ were predominantly found in the nucleus. All subunits of arterivirus nsp1 contained the IFN suppressive activity and inhibited both interferon regulatory factor 3 (IRF3) and NF-κB mediated IFN promoter activities. Similar to PRRSV–nsp1α, CBP degradation was evident in cells expressing LDV–nsp1α and SHFV–nsp1γ, but no such degradation was observed for EAV–nsp1. Regardless of CBP degradation, all subunits of arterivirus nsp1 suppressed the IFN-sensitive response element (ISRE)-promoter activities. Our data show that the nsp1-mediated IFN modulation is a common strategy for all arteriviruses but their mechanism of action may differ from each other.

Introduction

The family *Arterividae* in the order *Nidovirales* consists of a group of enveloped, single-stranded, positive-sense RNA viruses including porcine reproductive and respiratory syndrome virus (PRRSV), lactate dehydrogenase-elevating virus (LDV) of mice, equine arteritis virus (EAV), and simian hemorrhagic fever virus (SHFV). The arterivirus genome varies between 12.7 and 15.7 kb in length but their genome organization is relatively consistent with some minor variations (Snijder et al., 2013). At least 10 functional open reading frames (ORFs) have been identified in the PRRSV genome: ORF1a, ORF1b, ORF2a, ORF2b, and ORFs 3 through 7, plus recently identified ORF5a within ORF5 (Firth et al., 2011; Johnson et al., 2011; Meulenberg et al., 1993; Snijder et al., 1999; Wootton et al., 2000). For SHFV, four additional ORFs (2a, 2b, 3, and 4) immediately downstream of the replicase gene are duplicated (Godeny et al., 1998), and the gene duplication was confirmed in four (krc1, krc2, krtg1, krtg2) newly identified SHFV isolates (Lauck et al., 2011, 2013). In addition, a -2 ribosomal frame-shifting has been reported for expression of transframe (TF) ORF in the nsp2-coding region, and TF ORF is conserved in PRRSV, LDV and SHFV (Fang et al., 2012). The structural proteins encoded by ORFs 2a through 7 are expressed from the 3′-co-terminal nested set of subgenomic (sg) mRNAs (Firth et al., 2011; Godeny et al., 1998; Johnson et al., 2011; Meulenberg et al., 1993; Snijder et al., 1999). Mediated by the -1 frame-shifting in the ORF1a/ORF1b overlapping region, two polyproteins pp1a and pp1ab are synthesized (den Boon et al., 1991), and these polyproteins are proteolytically processed by two papain-like cysteine proteinases (PLPs) 1α and 1β in nsp1, a papain-like proteinase (PLP2) in nsp2, and a serine

* Corresponding author. Tel.: +1 217 244 9120.
E-mail address: dyoo@illinois.edu (D. Yoo).

http://dx.doi.org/10.1016/j.virol.2014.04.028
0042-6822/

protease (SP) in nsp4. Thus, the proteolytic processing of pp1a and pp1ab generates 13 nsps for EAV and 14 nsps for PRRSV and LDV (reviewed by Fang and Snijder, 2010; Snijder et al., 2013).

Arterivirus nsp1 is a multifunctional regulatory protein. For EAV, nsp1 is thought to regulate the accumulation of the viral genomic RNA and subgenomic (sg) mRNAs in a manner by determining the levels at which their negative-stranded templates are produced (Nedialkova et al., 2010). The N-terminal zinc finger (ZF) domain was essential for this function (Tijms et al., 2001). Arterivirus nsp1 harbors several important motifs: two motifs of PLP1α and PLP1β, two zinc finger motifs of ZF1 and ZF2, and a nuclease domain (Xue et al., 2010; reviewed in Fang and Snijder, 2010; Snijder et al., 2013). The PLP1α and PLP1β sequence motifs are relatively well conserved among nsp1 of arteriviruses with some functional variations. Both PLP1α and PLP1β motifs are found in nsp1 of PRRSV, LDV and EAV, but for EAV, PLP1α is inactive whereas PLP1β remains functional (den Boon et al., 1995; Ziebuhr et al., 2000). The PLP1α activity directs the internal cleavage of nsp1 to produce nsp1α, and the PLP1β activity is thought to release nsp1β from nsp2 of pp1a and pp1ab. In PRRSV, failure of the PLP1α-mediated nsp1 cleavage impairs the synthesis of viral mRNA but does not affect the genome replication. In contrast, no evidence of viral RNA synthesis was detected in PLP1β-impaired PRRSV mutants, indicating that the correct cleavage of nsp1β from nsp2 is essential for PRRSV genome replication (Kroese et al., 2008). Interestingly, the protease activities of PRRSV nsp1α and PRRSV nsp1β become inactive once cleaved due to the stable cohesion between the C-terminal extensions (CTE) and PLP1 motifs according to the X-ray crystallographic studies (Sun et al., 2009; Xue et al., 2010). The functional existence of ZF1 at the N-terminal region of nsp1 has been confirmed for EAV, and the presence of ZF2 in the C-terminal region of nsp1α has been described for PRRSV (Sun et al., 2009; Tijms et al., 2001). For SHFV, the nsp1 sequence reveals an array of three potential domains for PLP1α, PLP1β, and PLP1γ (Snijder et al., 2013), but these motifs have not experimentally been confirmed for their function.

Restricted tropism of arteriviruses limits their host range to suids, mice, equids, and non-human primates for PRRSV, LDV, EAV, and SHFV, respectively, and macrophages appear to be the primary target cells for their infections (Snijder and Meulenberg, 1998). Arteriviruses establish persistent infection in certain circumstances, and LDV in particular causes a life-long persistence in infected mice (Anderson et al., 1995; Plagemann et al., 1995). Arteriviruses seem to have evolved to escape the host immune surveillance and suppress the antiviral response. The type I interferon (IFN) system is a key component of the innate immunity and represents the first lines of defense against virus infection (Samuel, 2001). Subsequently, antiviral actions from IFN-stimulated gene (ISG) expression contribute to the antiviral state of cells (Sadler and Williams, 2008). For PRRSV however, IFN production is negligible in virus-infected cells and pigs, and the virus seems to suppress the IFN cascade (Albina et al., 1998). The molecular basis for IFN suppression by PRRSV has recently been explored and at least five viral proteins has been identified as an IFN antagonist, which includes four non-structural proteins (nsp1α, nsp1β, nsp2, and nsp11) and a structural protein (nucleocapsid, N) (Reviewed in Sun et al., 2012; Yoo et al., 2010).

Extensive studies have accentuated nsp1α and nsp1β as IFN modulators for PRRSV, and the inhibition of both IFN production and JAK-STAT (Janus Kinase-Signal Transducers and Activators of Transcription) signaling pathways have been shown in virus-infected cells and gene-transfected cells (Yoo et al., 2010; Sun et al., 2012). Both IRF3-mediated and NF-κB-mediated IFN production pathways are affected by nsp1α and nsp1β (Beura et al., 2010; Chen et al., 2010; Song et al., 2010), and the functional domains have been identified (Beura et al., 2012; Han et al., 2013; Li et al., 2013). It was reported that PRRSV nsp1α reduced the NF-κB activity (Song et al., 2010), and also nsp1α degrades the cyclic AMP responsive element binding (CREB)-binding protein (CBP) in a proteasome-dependent manner, leading to the suppression of IFN production (Han et al., 2013). In contrast, PRRSV nsp1β degrades karyopherin-α1 (KPNA1) and blocks nuclear translocation of interferon-stimulated gene factor 3 (ISGF3) (Patel et al., 2010; Wang et al., 2013). Besides PRRSV, no such study has been conducted for other member viruses in the family Arteriviridae. In the current study, we have investigated the biogenesis of nsp1 of arteriviruses and the role of nsp1 cleavage products for IFN synthesis and suppression. We report that the IFN modulation by nsp1 is a common strategy in arteriviruses for immune modulation. The molecular bases of immune evasion however may differ among arteriviruses.

Results

PLP domains in SHFV–nsp1

Two separate PLP domains, PLP1α and PLP1β, have been identified in nsp1 of PRRSV. These domains consist of catalytic residues C76 and H146, and C270 and H339, respectively. Both PLP1α and PLP1β domains are functional and generate nsp1α and nsp1β, respectively (Sun et al., 2009; Xue et al., 2010). For LDV, PLP domains in nsp1 resemble those of nsp1 of PRRSV, and their activities and cleavages may likely mimic those of PRRSV–nsp1. For EAV, PLP1α is composed of K73 and H122, and the K–H motif instead of the C–H motif in PRRSV has been shown to be inactive. As a result, EAV–nsp1α is not cleaved off from EAV–nsp1β, and thus uncleaved nsp1 is produced by the PLP1β activity (den Boon et al., 1995; Snijder et al., 1992). For SHFV, three potential PLP domains (PLP1α, PLP1β, and PLP1γ) are found according to sequence comparisons and each domain is presumed to be functional to generate nsp1α, nsp1β, and nsp1γ, respectively (Fig. 1A). The SHFV–PLP1α domain consists of C115 and H130, and resembles PRRSV–PLP1α and LDV–PLP1α. SHFV–PLP1β however is rather similar to SHFV–PLP1γ, suggesting gene duplication. Both SHFV–PLP1β and SHFV–PLP1γ are aligned well with PRRSV–PLP1β, LDV–PLP1β, and EAV–PLP1β (Fig. 1B).

To examine the cleavage products of nsp1 for each arterivirus, nsp1 genes were individually cloned and expressed in cells (Fig. 1D). A FLAG-tag was added to the N-terminus of each construct and thus only N-terminal cleavage product would be detected when using anti-FLAG antibody. LDV–nsp1α was identified as a 22 kD protein (lane 2), and the molecular size was slightly larger than 21 kD of PRRSV–nsp1α (lane 1), reflecting the predicted molecular weights of 21.1 kD and 20.8 kD for LDV–nsp1α and PRRSV–nsp1α, respectively. EAV–nsp1 was detected as a 30 kD protein (lane 3). In cells expressing SHFV–nsp1, a 39 kD protein was observed (Fig. 1D, lane 4), which was much larger than the predicted size of 21 kD for SHFV–nsp1α and was rather similar to the sum of nsp1α and nsp1β. This result suggests that the SHFV–PLP1α domain may be non-functional and instead SHFV–PLP1β cleaves off SHFV–nsp1β to generate a single protein of nsp1α and nsp1β.

To confirm the proteolytic activity of each PLP of SHFV–nsp1, different sets of nsp1 constructs were made using a FLAG tag at the N-terminus of each construct (Fig. 2A, left panel). Then, either single or double amino acid mutations were introduced to the catalytic sites to subvert the function of respective PLP. PRRSV–nsp1 and PRRSV–nsp1α were included as a cleavage control. To determine the enzymatic activity of SHFV–PLP1α, individual constructs were transfected to cells for 24 h and their cleavage patterns were examined using anti-FLAG antibody. To exclude

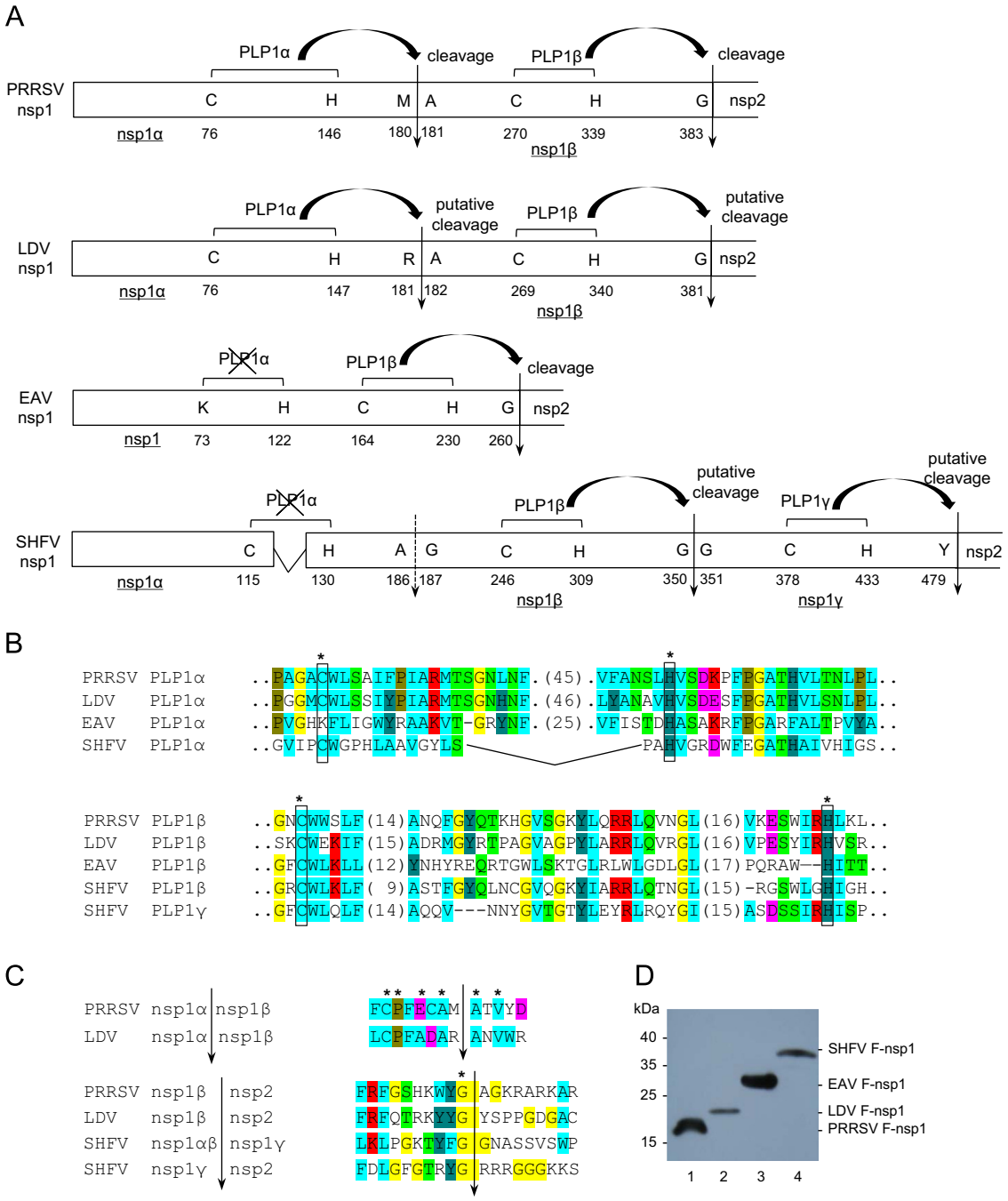

Fig. 1. Schematic presentation and sequence alignments of arterivirus nsp1. (A) Structures and potential cleavage sites of nsp1 of PRRSV, LDV, EAV, and SHFV. The nsp1 protein for PRRSV, LDV, EAV, and SHFV is of 383, 381, 260, and 479 amino acids (aa), respectively. The catalytic residues for PLPs are indicated. Solid vertical arrows represent the PLP-mediated cleavage sites and dotted arrows indicate predicted cleavage sites. Crossing-outs indicate non-functional PLPs. Numbers indicate amino acid positions in nsp1. The space between aa positions 115 and 130 in SHFV–nsp1 indicates a deletion within the PLP1α domain in arteriviruses. (B) Multiple sequence alignments of the PLP domains of nsp1 of arteriviruses. Conserved residues are shown in colors. PLP catalytic sites are boxed and indicated with asterisks. Dotted and solid lines indicate amino acid deletions. Numbers in parenthesis indicate the numbers of amino acids between the two sequences. (C) Sequence alignments of PLP-directed cleavage sites in nsp1 of different arteriviruses. Conserved amino acid residues are indicated in asterisks. Vertical arrows indicate cleavage sites. Sequence alignments were constructed using Clustal X2.1 and presented in reference to the previous report (van Hemert and Snijder, 2007). (D) Identification of the N-terminal cleavage product of individual arterivirus nsp1. Individual nsp1 genes were FLAG-tagged at their N-terminus and transiently expressed in cells followed by SDS-PAGE and Western blot using anti-FLAG antibody.

a possible influence by the N-terminal tag on the PLP1α activity, a C-terminal-tagged construct was made and designated SHFV–nsp1αβ/F. The nsp1αAA/β mutant was made to destroy the PLP1α motif by substituting C115 and H130 to C115A and H130A, respectively. After transfection, cell lysates were prepared and subjected to Western blot using FLAG antibody. SHFV–nsp1α and SHFV–nsp1β were expressed as 21 kD and 18 kD proteins, respectively (Fig. 2A, right panel, lanes 4, 5). Expressions of SHFV–nsp1, SHFV–nsp1αβ, SHFV–nsp1αβ/F, and SHFV–nsp1αAA/β produced a 39 kD protein which was the sum of nsp1α and nsp1β (lanes 6, 7, 8, 9), demonstrating that the cleavage did not occur between nsp1α and nsp1β, and suggesting that SHFV–PLP1α was most likely inactive.

To study the role of PLP1β, SHFV–nsp1β/γ and three additional PLP1β mutants (nsp1βAH/γ, nsp1βCA/γ, and nsp1βAA/γ) were constructed (Fig. 2B, left panel). When they were expressed

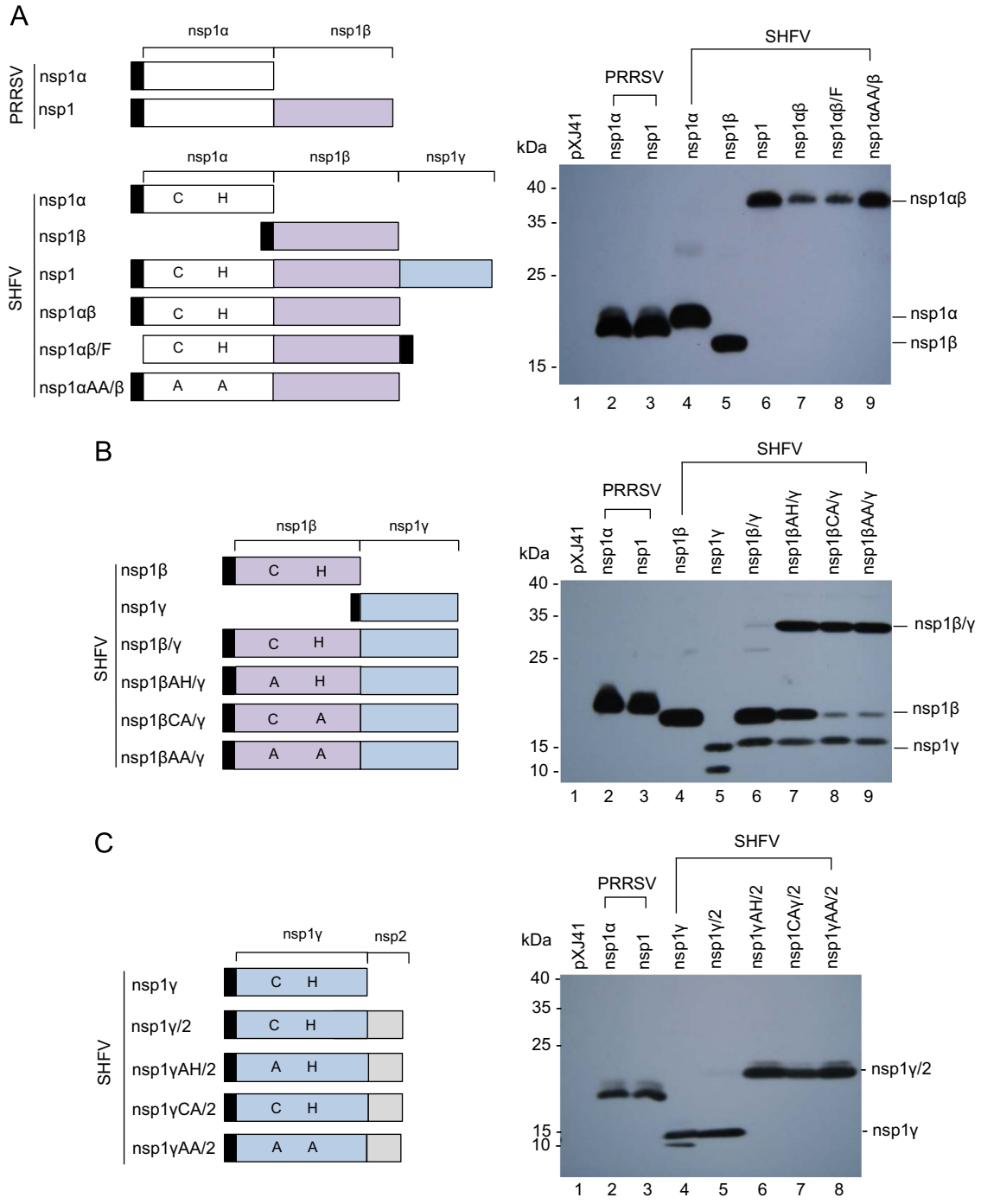

Fig. 2. PLP-mediated cleavages of SHFV–nsp1. (A) Structural illustration and self-cleavage of SHFV–nsp1 mutants and PLP1α mutants. Each construct was fused with a FLAG tag (dark areas) at the N-terminus or C-terminus. C and H residues of the catalytic dyad of PLP1α and alanine substitution are indicated (left panel). HeLa cells were transfected with indicated constructs for 24 h, and cell lysates were subjected to Western blot using anti-FLAG antibody. 21 kD, 18 kD, and 31 kD proteins represent SHFV–nsp1α, SHFV–nsp1β, and SHFV–nsp1α/β constructs, respectively (right panel). (B) Identification of SHFV–PLP1β mediated cleavage products. Schematic diagrams for constructs to determine PLP1β-mediated cleavages were shown in the left panel. 33 kD, 18 kD, and 15 kD proteins represent an uncleaved form of SHFV–nsp1β/γ, SHFV–nsp1β, and SHFV–nsp1γ, respectively (right panel). (C) Generation of PLP1γ-mediated nsp1γ. Structural presentations of nsp1γ constructs were shown (left panel). nsp1γ was extended to include a partial sequence of nsp2. 15 kD protein represents nsp1γ and 23 kD protein represent an uncleaved form of nsp1γ/2 P (right panel).

in cells, an 18 kD protein was identified in SHFV–nsp1β/γ expressing cells (Fig. 2B, right panel, lane 6), and it resembled the predicted size of SHFV–nsp1β (Fig. 2B, right panel, lane 4), indicating that PLP1β was enzymatically functional to release SHFV–nsp1β from SHFV–nsp1. In contrast, a 33 kD protein was identified in PLP1β mutants expressing cells, and this size was consistent with the predicted size of the sum of nsp1β and nsp1γ (Fig. 2B, right panel, lanes 7–9). The 10 kD protein in lane 5 is an N-terminal cleavage product of SHFV–nsp1γ. This finding shows that the PLP1β activity was responsible for the generation of SHFV–nsp1β. Taken altogether, our data showed that SHFV–PLP1α was non-functional and thus SHFV–nsp1 was cleaved by PLP1β in between nsp1αβ and nsp1γ, and so only two cleavage products were generated from SHFV–nsp1. We designated the N-

terminal cleavage product of nsp1 as SHFV–nsp1αβ for the following studies.

To study the role of SHFV–PLP1γ for the nsp1↓nsp2 cleavage, the nsp1γ gene was fused with the 5′ partial sequence of nsp2, which was then named SHFV–nsp1γ/2P. Three mutants of PLP1γ (nsp1γAH/2P, nsp1γCA/2P, and nsp1γAA/2P) were constructed to destroy the potential PLP1γ activity by replacing catalytic amino acids (Fig. 2C, left panel). A 15 kD band was identified in SHFV–nsp1γ expressing and SHFV–nsp1γ/2P expressing cells (Fig. 2C, right panel, lanes 4, 5). In contrast, in PLP1γ mutants expressing cells, a 23 kD protein was identified (Fig. 2C, right panel, lanes 6–8). This size was the sum of nsp1γ and the 5′ terminal partial sequence of nsp2. These results indicate that the SHFV–PLP1γ domain was functional and cleaved the sequence between nsp1↓nsp2 for the generation of nsp1γ.

PLP-specific cleavages of SHFV–nsp1

Since PLP1α was functional for PRRSV and LDV but non-functional for EAV and SHFV, sequence specificity of the nsp1α–nspβ cleavage sites were examined for PRRSV and LDV (Fig. 1C, upper panel). CPFxxAxAT(N)V was identified as a consensus sequence, in which x for any amino acids. Since the PRRSV–PLP1α-mediated nsp1 cleavage occurs at M180↓A181, the cleavage site for LDV–PLP1α was predicted to R181↓A182 which is an immediate upstream of the second 'A' (Sun et al., 2009). Previously, the nsp1↓nsp2 cleavage sites were determined to G260↓G261 for EAV and G383↓A384 for PRRSV (Snijder et al., 1992; Xue et al., 2010). Both the SHFV–PLP1β and SHFV–PLP1γ sequences were aligned well with the PLP1β sequence of PRRSV, LDV, and EAV (Fig. 1B), and thus based on the sequence similarities, the cleavages sites by SHFV–PLP1β and SHFV–PLP1γ were relatively easily predictable. A consensus sequence of H(R/K)K(T)Y(W)Y(F)G was identified at the C-terminal region of PRRSV–nsp1β, LDV–nsp1β, and SHFV–nsp1αβ (Fig. 1C, lower panel), and because the PRRSV–PLP1β cleavage occurs immediately after G383, the LDV–PLP1β and SHFV–PLP1β cleavage sites were predicted to G381↓Y382 and G350↓G351, respectively. For SHFV–PLP1γ, the C-terminal four amino acid residues of SHFV–nsp1γ were highly conserved with the arterivirus consensus sequence, and thus the cleavage site by PLP1γ was predicted to G480↓R481 (Fig. 1C). To confirm the cleavage by SHFV–PLP1β and SHFV–PLP1γ, mutations were introduced to substitute G350, G351, Y479, G480, and R481 to either serine (S) or valine (V) (Fig. 3A and B, left panels). Y479 served as a functionally silent control. Cleavage of the mutant constructs was then analyzed by expressing each construct in cells followed by Western blot using anti-FLAG antibody. Compared to PLP1β cleavage of nsp1β/γ (Fig. 3A, right panel, lane 3), mutants nsp1βAA/γ, G350S, G350V, and G351V (Fig. 3A, right panel, lanes, 4–7) were less effective for cleaving nsp1 whereas G351S as a silent control efficiently released nsp1γ as anticipated (Fig. 3B, right panel, lane 8). These findings support the cleavage of G350↓G351 by PLP1β. To further determine the PLP1γ cleavage, the mutants Y479S, Y479V, G480S, G480V, R481S, and R481V were made and examined. No cleavage was found for Y479S, G480S, and G480V (Fig. 3B, right lane 5, 7 and 8), and the size of the uncleaved protein was identical to the size of nsp1γAA/2P (Fig. 3B, right panel, lane 4). A full cleavage of SHFV–nsp1γ/2P was observed for Y479V (Fig. 3B, right panel, lane 6) suggesting Y to V substitution at position 479 did not block the cleavage by PLP1γ. The SHFV–nsp1γ subunit was normally produced by any substitution of R481, R481S, and R481V (Fig. 3B, right panel, lanes 9 and 10), supporting the cleavage site by PLP1γ as Y479↓G480. The extra band above nsp1γ became visible when exposure time was extended, and this band also appeared in PRRSV–nsp1α, LDV–nsp1α, and SHFV–nsp1γAA/2P (Fig. 3B). The nature of this band was unclear.

Cellular localization of arterivirus nsp1 individual subunits

PRRSV–nsp1α is a nuclear–cytoplasmic protein distributed in the both nucleus and cytoplasm, whereas PRRSV–nsp1β and EAV–nsp1 are predominantly found in the nuclear and perinuclear regions (Li et al., 2012; Chen et al., 2010; Song et al., 2010; Tijms et al., 2002). Thus, it was of interest to determine the cellular distribution of each subunit of LDV–nsp1 and SHFV–nsp1. Plasmids coding for individual subunits of nsp1 were transfected into MARC-145 or HeLa cells for 24 h, and the subcellular distribution of each nsp subunit was determined by staining with anti-FLAG antibody (Table 3). LDV–nsp1α was localized in the both nucleus and cytoplasm (Fig. 4A, panel G), and its distribution patterns were similar to those of PRRSV–nsp1α (Fig. 4A, panel A). A predominant nuclear distribution was observed for LDV–nsp1β, SHFV–nsp1αβ, and SHFV–nsp1γ (Fig. 4A, panels M, P, S). For SHFV–nsp1αβ in particular, three staining patterns were observed: perinuclear staining (Fig.4B, A-type), nuclear aggregation (Fig.4B, B-type), and predominantly nuclear staining (Fig.4B, C-type). In HeLa cells, 74% of cells showed A-type staining and 10% of cells appeared to be of C-type (Fig. 4C, upper panel, black bars). In MARC-145 cells, the A-type staining pattern decreased to 54% while B-type staining increased to 38% and C-type to be 8% (Fig. 4C, upper). For SHFV–nsp1γ, a majority of cells (74%) showed A-type staining in HeLa cells (Fig. 4C, lower), whereas in MARC-145 cells, three patterns were relatively evenly distributed by 30% each, suggesting a possible variation of their roles depending on cell types.

Suppression of IFN production by nsp1 subunits of arteriviruses

Both PRRSV–nsp1α and PRRSV–nsp1β have been reported to participate in the suppression of IFN production, and thus it was of interest to determine whether nsp1 of other arteriviruses plays a similar role to antagonize the IFN activity. To examine this possibility, a luciferase reporter assay was employed. Plasmids coding for individual subunits of different arterivirus nsp1 were individually co-transfected with the reporter plasmids, followed by poly(I:C) stimulation for IFN induction. Virtually all subunits exhibited comparable levels of IFN responses to those of PRRSV–nsp1α and PRRSV–nsp1β (Fig. 5A, left panel). Similar to IFNβ–Luc, every subunit of arterivirus nsp1 showed the suppression of IRF3–Luc activity (Fig. 5A, middle panel) and NF-κB–Luc activity (Fig. 5A, right panel). To further confirm the suppression of IFN by nsp1, an IFN bioassay was conducted using vesicular stomatitis Indiana virus expressing GFP (VSIV-GFP). HeLa cells were transfected with a plasmid expressing each of the nsp1 subunit gene, and then stimulated with poly(I:C). The supernatants were collected, serially-diluted, and incubated with MARC-145 cells. After incubation, cells were infected with VSIV-GFP. The presence of IFN in the supernatant will inhibit the replication of VSIV-GFP, resulting in the absence of GFP expression. If IFN suppression occurs by arterivirus nsp1, a reduced amount of IFN secreted in the supernatants will allow the replication of VSIV-GFP and so the GFP expression will be visible. In the present study, two folds-dilution of supernatant exhibiting the minimum 50% GFP expression was calculated as the end point for IFN-directed inhibition of VSIV replication. Cells transfected with the empty vector pXJ4 or pXJ41-GST and stimulated with poly(I:C) resulted in efficient production of IFN in the supernatant, and the VSIV-GFP replication was inhibited as anticipated. For this control, the end point for GFP expression was determined as 1:16 (Fig. 5B, second and third panels from top). Cells transfected with pXJ41 without stimulation resulted in the absence of IFN production, and thus VSIV-GFP did replicate normally and the end point was determined as 1 (Fig. 5B, top panels). Cells incubated with the supernatant from nsp1 subunit-expressing cells showed a very little inhibition of VSIV-GFP and the end point was determined to be 1:2 for each of the

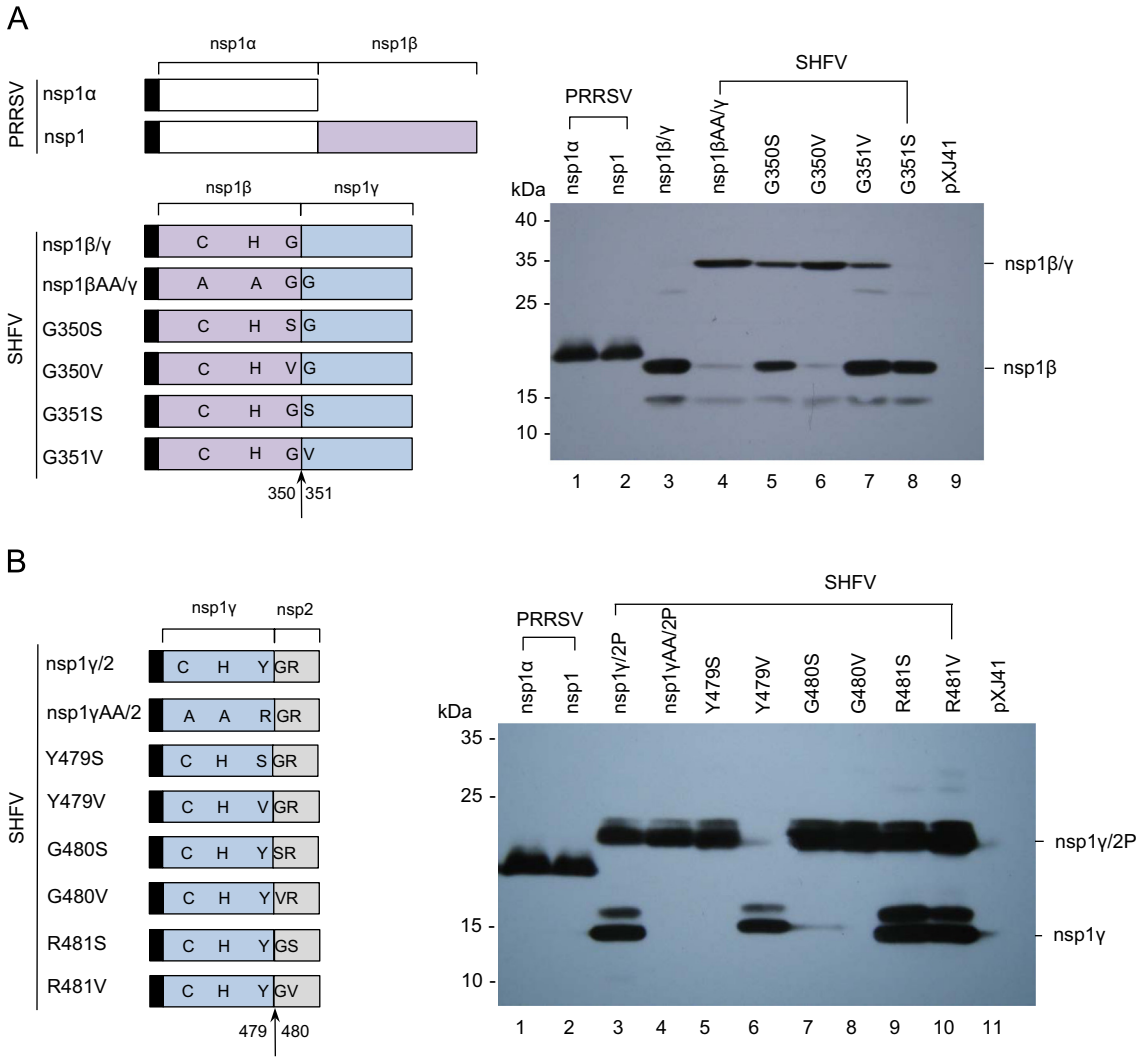

Fig. 3. Identification of PLP1β-directed and PLP1γ-directed cleavages of SHFV–nsp1. (A) Identification of PLP1β-directed cleavage products of SHFV–nsp1. Each construct was fused with a FLAG tag at the N-terminus (dark areas). The catalytic residues of PLP1β and their amino acid substitutions are indicated. PLP1β-directed nsp1 cleavage was predicted at G350↓G351 (arrows), and a mutation to G350S, G350V, G351S, or G351V is indicated (left panel). HeLa cells were transfected with individual constructs illustrated in the left panel for 24 h, and cell lysates were subjected to Western blot using anti-FLAG antibody. The 33 kD band represents the uncleaved nsp1β/γ protein and the 18 kD band represents the nsp1β subunit (right panel). (B) Identification of PLP1γ-directed nsp1 cleavage. Each construct for PLP1γ-directed nsp1 processing was fused with a FLAG tag at the N-terminus for detection by anti-FLAG antibody. The catalytic residues and amino acids at the junction of predicted cleavage sites between nsp1γ and nsp2 are indicated. These amino acids were subjected to substitution by G or S (left panel). The 23 kD band indicates the uncleaved nsp1γ/2 P and the 15 kD band indicates the nsp1γ subunit (right panel).

subunits. The inhibition level was 8-folds lower than that of the control (1:16), indicating that each of nsp1 subunits strongly suppressed the IFN production in transfected cells (Fig. 5B). These observations were consistent with the luciferase assay data and demonstrate the IFN suppression by arterivirus nsp1 subunits.

Phosphorylation and nuclear translocation of IRF3 in the presence of nsp1 subunits

When stimulated for IFN induction, IRF3 is phosphorylated by IKKε and/or TBK1 kinases, and the phosphorylated IRF3 results in dimerization and conformational switch, exposing the nuclear localization signal (NLS) for subsequent translocation to the nucleus (Baccala et al., 2007). Some viral IFN antagonists degrade IRF3, inhibit IRF3 phosphorylation, or block IRF3 nuclear translocation (Ren et al., 2011; Sen et al., 2010; Zhu et al., 2011). Since our results showed the IRF3-mediated IFN suppression by nsp1 subunits, and because for PRRSV, nsp1α- and nsp1β-mediated IFN suppressions were IRF3-independent (Chen et al., 2010; Kim et al., 2010), it was of interest to examine whether IRF3 function was altered by nsp1 of other arteriviruses. The amounts of total IRF3 (Fig. 6A, middle panel) and phosphorylated IRF3 (pIRF3, Fig. 6A, upper panel) were examined after expression of individual subunits of nsp1. No significant changes were observed for levels of IRF3 and pIRF3 in comparison to those of control, suggesting that IRF3 inhibition occurred at steps after phosphorylation. We thus explored the nuclear localization of IRF3 by cell fractionation (Fig. 6B) and fluorescence staining (Fig. 6C). After poly(I:C) stimulation, IRF3 was partly accumulated in the nuclear fraction, and this was not affected by expression of nsp1 subunits (Fig. 6B, right upper panel). HSP90 and PARP as the cytosolic and nuclear proteins markers, respectively, remained in their respective compartments (Fig. 6B, middle upper panel, lanes 1–9; middle lower panel, lanes 10–18), indicating that the results were not due to the cross-contamination during fractionation. To confirm the cell fractionation result, immunofluorescence of endogenous IRF3 was conducted after poly(I:C) stimulation. Without stimulation, IRF3 was distributed normally in the cytoplasm with some nuclear diffusion (Fig. 6C, panel A), but when stimulated, it was translocated to the nucleus (Fig. 6C, panel D). In cells expressing the nsp1

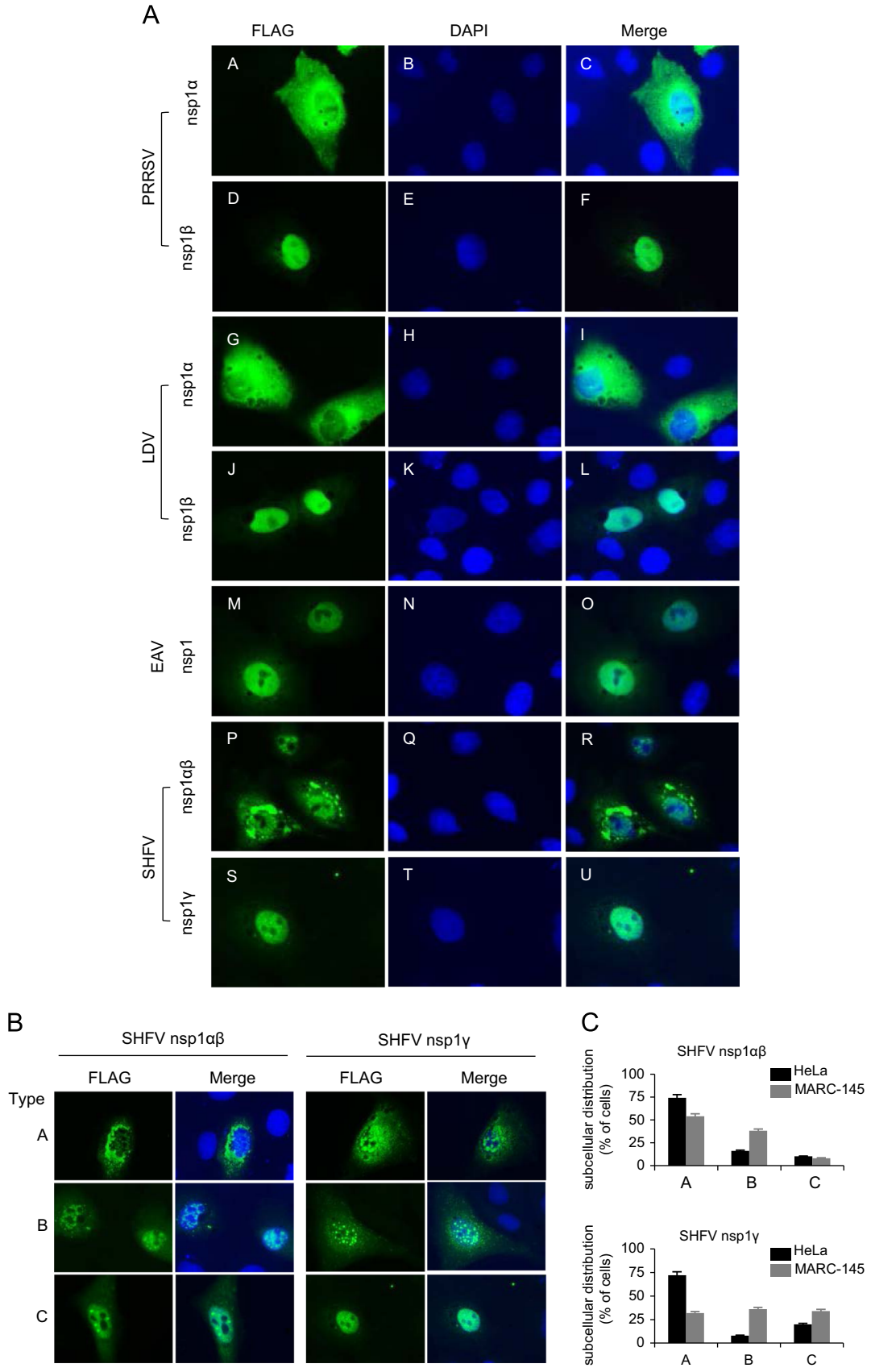

Fig. 4. Subcellular localization of nsp1 subunits of arteriviruses in HeLa and MARC-145 cells. (A) Cells were grown to 40% confluency and transfected with indicated genes for 24 h. Cells were fixed with 4% paraformaldehyde and stained with anti-FLAG Ab followed by staining with Alexa 488-labeled anti-mouse Ab and DAPI. Cellular localization of nsp1 subunits were examined by fluorescence microscopy. (B) Types of cellular distribution for SHFV–nsp1αβ and SHFV–nsp1γ. (C) The percentages of cells showing different types of subcellular distribution were calculated using the following formula; (Number of cells showing each of distribution types/(50 cells expressing SHFV–nsp1αβ or SHFV–nsp1γ) × 100.

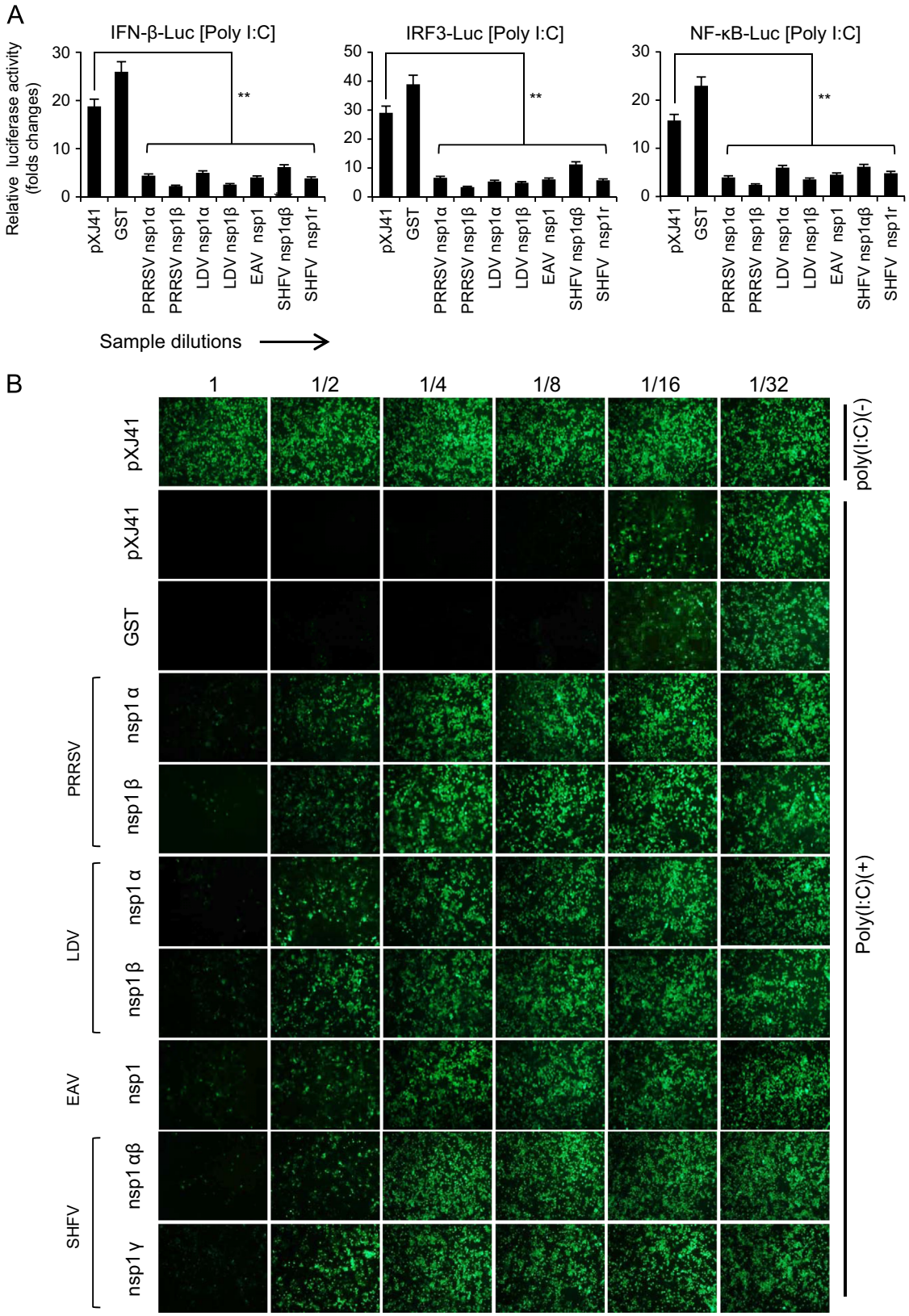

Fig. 5. Suppression of IFN-β production by individual arterivirus nsp1 subunits. (A) HeLa cells were seeded in 12-well plates and co-transfected with pIFN-β-Luc, p4 × IRF3–Luc, or pRD II-Luc, along with individual arterivirus nsp1 genes and pTK-RL as an internal control at a ratio of 1:1:0.1. At 24 h post-transfection, cells were stimulated with 1 μg/ml of poly(I:C) for 12 h, and lysed for the reporter determination using the Dual Luciferase assay system (Promega). Relative luciferase activities were calculated by normalizing the firefly luciferase to renilla luciferase activities according to the manufacturer's protocol. The data represent the means of three independent experiments, each experiment in triplicate. Statistical significance in fold changes of relative luciferase activity are indicated as follows: $^{*}P < 0.05$, and $^{***}P < 0.01$. (B) IFN bioassay using vesicular stomatitis Indiana virus(VSIV)-GFP. HeLa cells in 6-well plates were transfected with individual arterivirus nsp1 subunit genes for 24 h, and stimulated with poly(I:C) for 12 h. Cell culture supernatants were collected and diluted serially by 2-folds. MARC-145 cells were grown in 96-well plates and incubated with each dilution of supernatants for 24 h, and then infected with VSIV-GFP at an MOI of 0.1 for 16 h. VSIV replication was measured by monitoring the fluorescence by GFP expression.

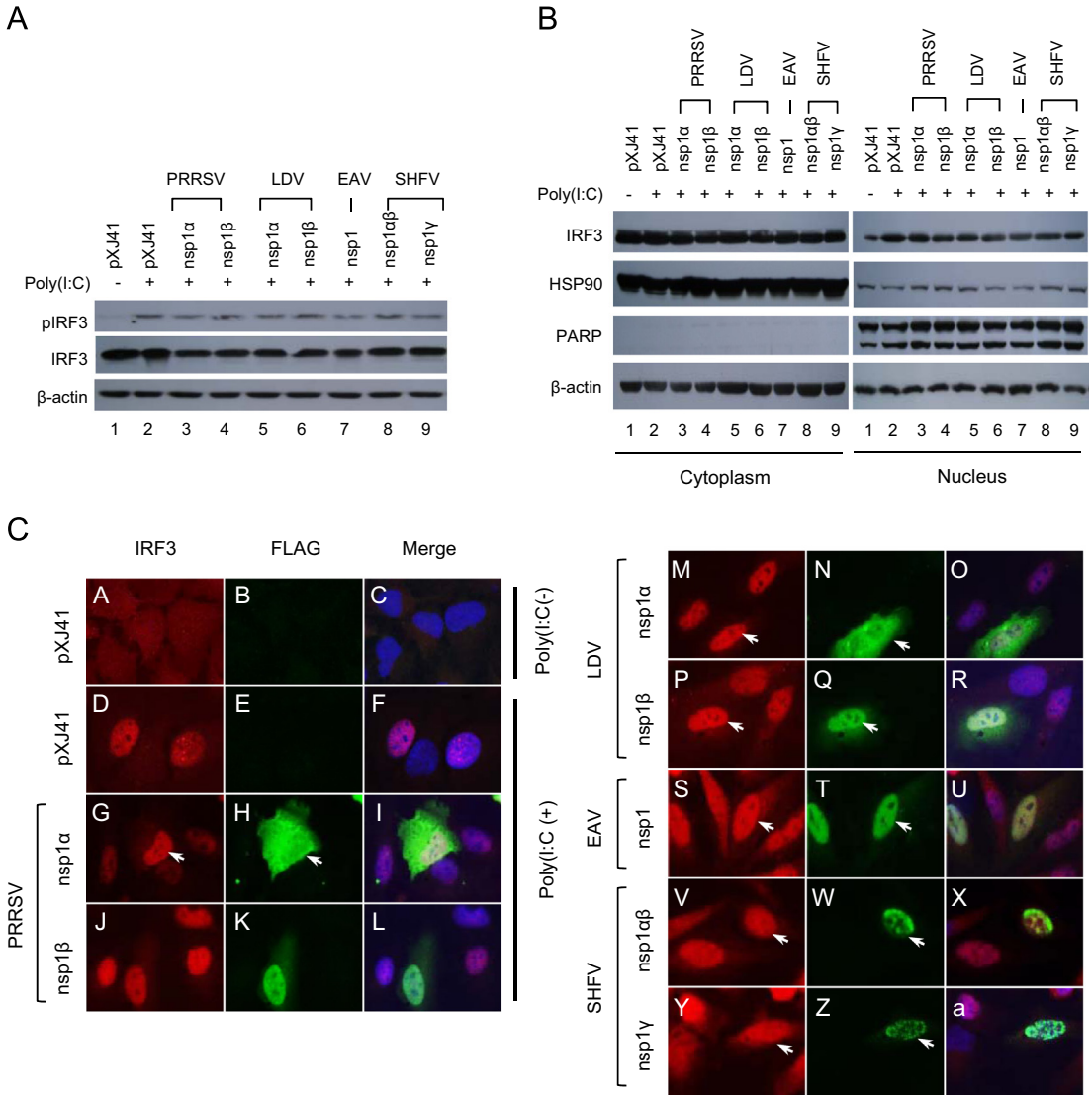

Fig. 6. Activation and nuclear localization of IRF3 in cells expressing the individual arterivirus nsp1 subunits. (A) Phosphorylation of IRF3 in the presence of arterivirus nsp1 subunits. HeLa cells were transfected with plasmids expressing each of individual arterivirus nsp1 subunits for 24 h and stimulated by poly(I:C) for 8 h. Cells were lysed and subjected to Western blot using phospho-IRF3 (Ser396) antibody (top panel), IRF3 antibody (second panel), and β-actin antibody (bottom panel). (B) Nuclear localization of IRF3 in cells expressing the individual arterivirus nsp1 subunits. HeLa cells expressing individual nsp1 subunits were fractionated followed by Western blot using IRF3 antibody (upper panel), anti-HSP90 antibody as a cytosolic marker (second panel), anti-PARP antibody as a nuclear protein marker (third panel), and β-actin antibody as a loading control (bottom panel). (C) Nuclear translocation of IRF3 in nsp1 subunit- gene transfected cells. Cells were stimulated with poly(I:C) for 8 h, fixed with 4% paraformaldehyde, and incubated with rabbit anti-IRF3 Ab and mouse anti-FLAG Ab, followed by incubation with Alexa Fluor 594-conjugated (red) and 488-conjugated (green) secondary antibodies, respectively, along with DAPI for nucleus staining (blue). pXJ41 is an empty vector and used as a control. Arrows indicate IRF3 and respective nsp1 subunit in the nucleus.

subunits (Fig. 6C, middle column, white arrows), IRF3 was found to normally translocate to the nucleus after stimulation (Fig. 6C, left column, white arrows). These results show that nsp1 did not affect IRF3-nuclear translocation, suggesting that the nsp1-mediated IFN suppression occurs downstream of IRF3 nuclear localization"

CBP degradation and nsp1 subunits

In our studies, all subunits of arterivirus nsp1 appear to suppress the IFN production. Since CBP is degraded by PRRSV–nsp1α in the nucleus (Han et al., 2013), we examined whether CBP degradation was a common mechanism in arteriviruses. For this, HeLa cells were transfected with plasmids expressing individual nsp1 subunits, and the CBP degradation was determined by immunofluorescence and Western blot assays (Fig. 7). PRRSV–nsp1α was used as a CBP degradation control and PRRSV–nsp1β was used as a negative control. LDV–nsp1α caused a notable reduction of CBP, and the level of reduction was comparable to that of PRRSV–nsp1α (Fig. 7A, lanes 2, 4). In cells expressing LDV–nsp1α and SHFV–nsp1γ, CBP degradation was also evident in immunofluorescence assay (Fig. 7B, panels M, c), even though SHFV–nsp1γ-mediated CBP degradation was less evident in Western blot. In contrast, no CBP degradation was observed for LDV–nsp1β (panel Q), EAV–nsp1 (panel U), and SHFV–nsp1αβ (panel Y). The CBP degradation was quantified by counting the numbers of cells exhibiting the reduced CBP and the number of cells expressing the respective nsp expression. Approximately 80% of cells expressing PRRSV–nsp1α and 78% of cells expressing LDV–nsp1α showed a significant reduction of CBP whereas only approximately 30% of cells expressing SHFV–nsp1γ exhibited the CBP reduction (Fig. 7C). Together with the data from Western blot, it further confirmed that LDV–nsp1α and SHFV–nsp1γ caused CBP degradation, resulting in the inhibition of enhanceosome formation and thus suppression of IFN production.

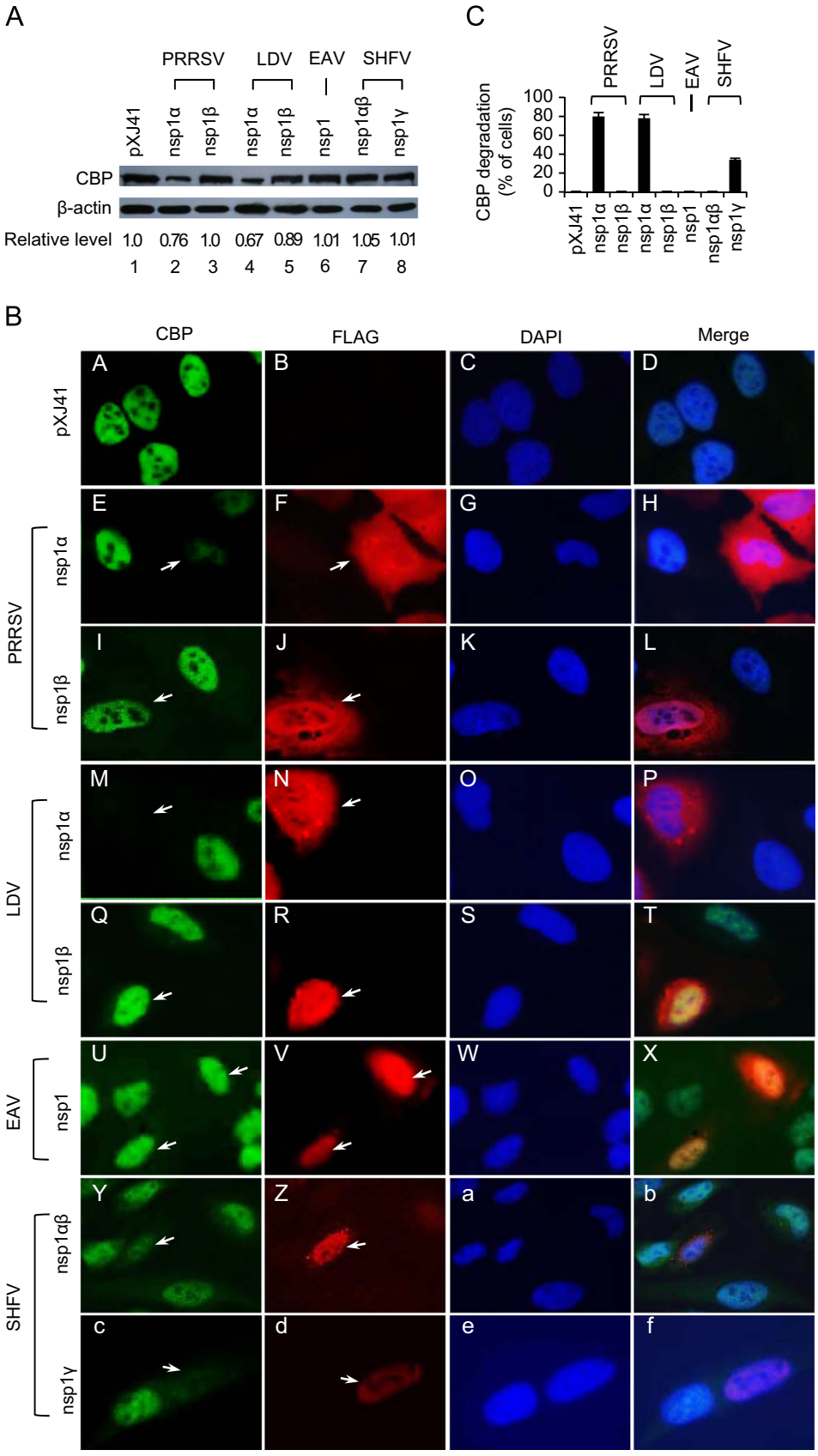

Fig. 7. Degradation of CBP by arterivirus nsp1 subunits. (A) HeLa cells were transfected with individual constructs expressing each of arterivirus nsp1 subunits for 24 h, and cell lysates were subjected to Western blot using anti-CBP antibody to examine the endogenous level of CBP (top panel). The CBP degradation was quantified and relative levels were shown below each lane. (B) Determination of CBP degradation by IFA. HeLa cells were grown to 40% confluency and transfected with individual arterivirus nsp1 subunit constructs. At 24 h, cells were co-stained with rabbit anti-FLAG Ab and mouse anti-CBP Ab, followed by incubation with Alexa Fluor 594-conjugated (red) and 488-conjugated (green) secondary antibodies, respectively, along with DAPI for nucleus staining (blue). Arrows indicate cells where CBP is degraded by nsp1. (C) The percentage of cells showing significant reduction of CBP was calculated using the following formula; (Number of cells showing more than 50% reduction of the CBP staining intensity compared to the control CBP staining intensity out of 50 nsp1-expressing cells/(50 cells expressing each subunits of arterivirus nsp1) × 100.

Suppression of ISRE by nsp1 subunits of arteriviruses

In addition to suppression of the IFN production pathway, PRRSV–nsp1α and PRRSV–nsp1β have been shown to suppress the JAK-STAT signaling pathway (Chen et al., 2010; Patel et al., 2010). We thus further examined whether nsp1 subunits of other arteriviruses would also suppress the IFN signaling. HeLa cells were co-transfected with a plasmid expressing individual subunit of arterivirus nsp1 and the ISRE-Luc reporter plasmid, followed by

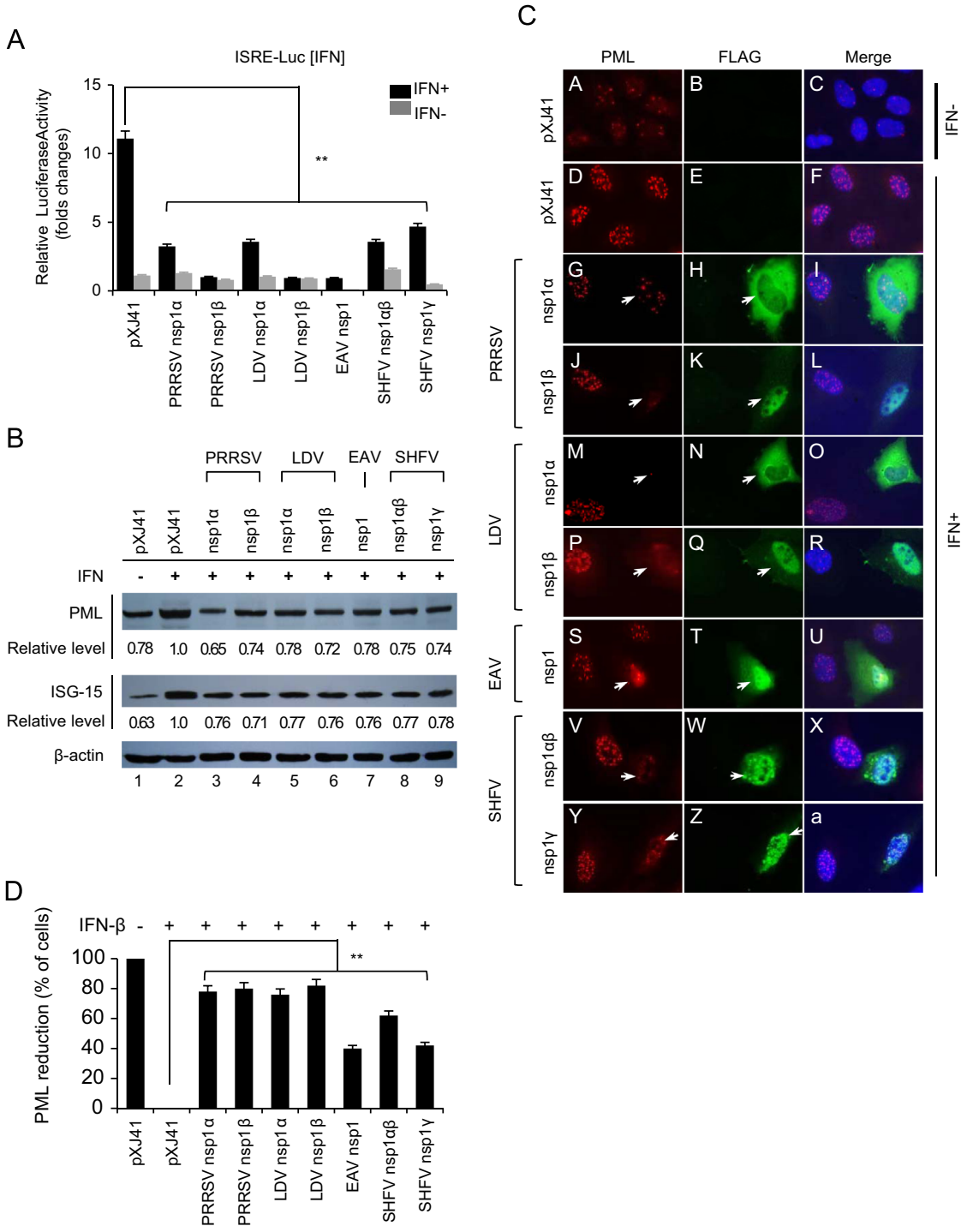

Fig. 8. Suppression of ISRE activities by arterivirus nsp1 subunits. (A) HeLa cells were co-transfected with 500 ng of pISRE-Luc, 500 ng of pXJ41 empty vector or a plasmid expressing individual arterivirus nsp1 subunit along with pTK-RL as an internal control. At 24 h post- transfection, cells were incubated with 1000 units/ml of IFN-β for 12 h, followed by luciferase reporter assays using the Dual Luciferase assay system (Promega). Relative luciferase activities were calculated by normalizing the firefly luciferase to renilla luciferase activities. Statistical significance in fold changes of relative luciferase activity between empty vector and each of the arterivirus nsp1 subunits is indicated as follows: $^{*}P < 0.05$, and $^{**}P < 0.01$. (B) HeLa cells were transfected with individual plasmids encoding nsp1 subunits for 24 h, followed by IFN treatment for 12 h. Cell lysates were subjected to Western blot analyses using anti-PML antibody (top panel) and anti-ISG15 antibody (second panel). β-actin was used as a loading control (bottom panel). (C) Reduced expression of PML in nsp1subunit-expressing cells. After IFN stimulation, cells were fixed with 4% paraformaldehyde and incubated with rabbit anti-FLAG Ab and mouse anti-CBP Ab for 2 h, followed by incubation with Alexa Fluor 594-conjugated (red) and Alexa Fluor 488-conjugated (green) secondary antibodies, respectively. The nuclei were stained with DAPI (blue). Arrows indicate the reduction of PML expression. Fold changes of PML and ISG-15 levels were shown below each of the images, respectively. (D) Percentage of cells showing reduced production of PML. Statistical significance is indicated as follows: $^{***}P < 0.01$.

stimulation with IFN-β. As shown in Fig. 8A, ISRE-dependent luciferase expression was suppressed by each subunit of all arteriviruses. To further confirm their suppressive effects on IFN stimulated gene (ISG) expression through the JAK-STAT pathway, ISG15 and promyelocytic leukemia (PML), whose expression is ISRE-dependent, were examined by Western blot (Fig. 8B; Chelbi-Alix et al., 1995). The reduction of ISG15 (middle panel, lanes 3 through 9) and PML (upper panel, lanes 3 through 9) was identified in cells expressing individual nsp1 subunit, in comparison to those in mock-transfected cells. The suppression of ISG15 expression by SHFV nsp1 was relatively weaker than those of PRRSV–nsp1β, LDV–nsp1β, and EAV–nsp1 but was still significant. The reduction of PML was also confirmed by the staining of nsp1-expressing cells (Fig. 8C). PML is a component of the nuclear bodies (NBs) (Dyck et al., 1994), and thus is stained as a punctate pattern in the nucleus. Compared to cells where no viral protein was expressed, the reduction of PML-NBs was evident in cells expressing PRRSV–nsp1α (panel G, arrow), PRRSV–nsp1β (panel J, arrow), LDV–nsp1α (Panel M, arrow), LDV–nsp1β (Panel P, arrow), EAV–nsp1 (panel S, arrow), SHFV–nsp1αβ (panel V, arrow), and SHFV–nsp1γ (panels Y, arrow). The reduction of PML was quantified by counting the number of cells exhibiting the reduced CBP out of 200 cells expressing viral nsp1 (Fig. 8D). Approximately, 80% of cells showed the reduction of PML-NBs for PRRSV–nsp1α, PRRSV–nsp1β, LDV–nsp1α, and LDV–nsp1β, whereas 60% of cells showed the reduction of PML-NBs for SHFV–nsp1αβ. In contrast, only 40% of cells showed the reduction of PML for EAV–nsp1 and SHFV–nsp1γ (Fig. 8D). Taken together, our results demonstrate that each subunit of all arterivirus nsp1 contained the inhibitory activity for ISRE and ISRE-dependent antiviral protein expression.

Discussion

During the processing of pp1a and pp1ab polyproteins in arteriviruses, PLP1α/β-mediated proteolytic cleavages are unique characteristics for nsp1 biogenesis, and the role of PLP1α/β for polyproteins processing and viral genome replication has been elucidated for PRRSV and EAV (For a review, see Fang and Snijder, 2010; Snijder et al., 2013). With an exception of SHFV, catalytic sites for nsp1 of other arteriviruses have been either predicted or confirmed by experiments (den Boon et al., 1995; Snijder et al., 1992). In the current study, we show that the processing of LDV–nsp1 is similar to that of PRRSV–nsp1, while SHFV–PLP1α in SHFV–nsp1 is non-functional as that of EAV–PLP1α. For EAV, the displacement of C73 by K73 in nsp1 explains the functional deficiency of PLP1α (Fig. 1A). For SHFV, two residues of C115 and H130 are critical for the catalytic activity of PLP1α, and these residues are conserved. However, a contiguous deletion of 55 amino acids is notable in the region between two catalytic residues of C115 and H130 when compared to PRRSV (Fig. 1A), thus likely contributing to the impaired function of SHFV–PLP1α.

To study the biogenesis of nsp1, the cleavage sites were first determined. The PRRSV–nsp1 cleavage site was initially predicted to Q166↓R167 in the case of North American genotype PRRSV or somewhere between Q166 and F173 for European genotype PRRSV (Allende et al., 1999; den Boon et al., 1995). Recent studies however, identified the cleavage at M180↓A181 for North American PRRSV, and similarly a corresponding site of H180↓S181 was predicted as the cleavage site for European genotype PRRV according to our sequence analysis (Chen et al., 2010; Sun et al., 2009). The discovery of authentic cleavage site results in addition of 14 amino acids to the C-terminus of PRRSV–nsp1α in contrast to the initial prediction. A crystallographic study shows that these additional 14 residues constitute the C-terminal extension (CTE) of PRRSV–nsp1α and are essential for formation of the newly described C-terminal zinc finger motif (Sun et al., 2009). We have previously shown that these 14 residues are essential for the nsp1α function for IFN suppression and cellular distribution (Song et al., 2010). Hence, keeping the structural integrity of nsp1α seems to be critical to retain its biological function for PRRSV replication. Thus, among the PLP1α homologs in arteriviruses, only PRRSV–PLP1α and LDV–PLP1α appear to be active and functional. When compared the nsp1α–nsp1β junction sequence of LDV to that of PRRSV, CPFxxAxAT(N)V (where x is any amino acid) is conserved between the two viruses, and thus, nsp1α↓nsp1β cleavage site for LDV–PLP1α is readily predictable. In fact, the junction sequence is highly conserved among LDV, PRRSV, and SHFV, and therefore, R181↓A182 is likely the correct cleavage site for LDV–PLP1α, and G381↓Y382 for LDV–PLP1β. Similarly, G350↓G351 is predicted to be the cleavage site for SHFV–PLP1β (Fig. 1C). According to our mutational studies, the cleavage site for SHFV–PLP1γ is reasonably predicted to Y479↓G480 rather than the previous prediction of G480↓R481.

It is intriguing that all subunits of arterivirus nsp1 have the ability to suppress the type I IFN production despite the limited sequence similarities. However, some critical functional motifs appeared to be conserved. The results from luciferase reporter assays indicate that either the IRF3-mediated or NF-κB-mediated signaling pathway are inhibited. In the current study, no changes were identified for both phosphorylation and nuclear localization of IRF3 in cells expressing arterivirus nsp1 subunits, which is in agreement with a previous study by Chen et al. (2010). Thus, it is proposed that the IFN inhibition by arterivirus nsp1 subunits may be a nuclear event. All subunits of arterivirus nsp1 are found to localize in the nucleus, but their role in the nucleus seems variable. PRRSV–nsp1α degrades CBP which is a crucial co-factor for IFN-β transcription (Han et al., 2013), and CBP degradation is also observed for LDV–nsp1α (Fig. 7). The subcellular distribution of PRRSV–nsp1α and LDV–nsp1α are both nuclear–cytoplasmic, and their distribution patterns are similar (Fig. 4). Since the PRRSV–nsp1α-mediated CBP degradation is a nuclear event and proteasome-dependent and also because of the lack of direct binding of PRRSV–nsp1α to CBP (Kim et al., 2010), the nuclear form of PRRSV–nsp1α is likely responsible for CBP degradation through utilizing a mediator or other signaling pathway to complete the degradation process.

In contrast to the nuclear–cytoplasmic distribution of nsp1α, PRRSV–nsp1β, LDV–nsp1β, and EAV–nsp1 are predominantly nuclear without cytoplasmic distribution (Table 3). IFN synthesis is inhibited by these proteins but a notable CBP degradation is absent, suggesting a novel strategy by nsp1β for IFN suppression. For SHFV–nsp1γ, CBP degradation was less pronounced but apparent by immunofluorescence in some SHFV–nsp1γ expressing cells, suggesting that a certain form of nsp1γ is probably responsible for CBP degradation. In addition to suppression of the IFN production pathway, all subunits of arterivirus nsp1 are found to inhibit the JAK-STAT signaling pathway. The basis for ISRE inhibition by LDV–nsp1α is similar to that of PRRSV–nsp1α as for CBP degradation. For PRRSV–nsp1β, the KPNA1 degradation has been reported to cause the inhibition of ISGF3 nuclear translocation thus to result in the inhibition of JAT-STAT pathway. Whether LDV–nsp1β and EAV–nsp1 also block the ISGF3 nuclear translocation remain to be determined. Different types of subcellular distribution are found for SHFV–nsp1αβ and SHFV–nsp1γ, suggesting that their nuclear localization is crucial for IFN suppression. The molecular basis for IFN suppression by SHFV–nsp1αβ and SHFV–nsp1γ needs to be further explored.

In summary, we have shown that the nsp1 subunits of all four arteriviruses are able to modulate the IFN production either through the production pathway or the signaling pathway, and their biological function seems to be corresponding to their cellular distributions. Taking together, nsp1 subunits of all viruses

in the family *Arteriviridae* are important IFN antagonists, and their IFN modulatory function seems to be a common strategy for evading the host immune system.

Materials and methods

Cells and viruses

HeLa cells (NIH AIDS Research and Reference Reagent Program, Germantown, MD) and MARC-145 cells (Kim et al., 1993) were grown in minimum essential medium (MEM) and Dulbecco's modified Eagle's medium (DMEM; Mediatech Inc., Manassas,VA), respectively, supplemented with 10% heat-inactivated fetal bovine serum (FBS; HyClone, Logan, UT) in a humidified incubator with 5% CO_2 at 37 °C. The PA8 strain of the North American genotype PRRSV (Wootton et al., 2000) was used. The full-length genomic sequence of PA8 shares 99.2% identity with the prototype PRRSV VR2332 of the North American genotype (Nelsen et al., 1999). Vesicular stomatitis virus (Indiana strain) expressing green fluorescent protein (VSV-GFP; Dalton and Rose, 2001) was kindly provided by Adolfo García-Sastre (Mt. Sinai School of Medicine, New York, NY). LDV was provided by Steve Jennings (Charles River Laboratories, Wilmington, MA). This virus was isolated from a mice breeding colony and designated LDV-Urbana. The SHFV nsp1 gene was cloned from the cDNA library provided by Eric Snijder (Leiden University Medical Center, Leiden, Netherlands). The nsp1 sequence from SHFV cDNA shared 99.2% nucleotide and 98.3% amino acid identity with the nsp1 sequence from GenBank (accession no.: NC_003092).The EAV nsp1 gene was cloned from the Bucyrus strain of EAV.

Antibodies and chemicals

Polyinosinic:polycytidylic [poly (I:C)], DAPI (4′,6-diamidino-2-phenylindol), anti-Flag MAb (F3165), and anti-FLAG PAb (F7425) were purchased from Sigma (St. Louis, MO). Anti-β-actin MAb (sc-47778), anti-CBP MAb (sc-7300), anti-IRF3 PAb (sc-9082), anti-HSP90 MAb (sc-69703), anti-PARP PAb (sc-7150) and anti-PML PAb (sc-5621) were purchased from Santa Cruz Biotechnologies Inc. (Santa Cruz, CA). Anti-ISG15 PAb was purchased from Thermo Scientific Pierce (Rockford, IL). Phospho-IRF-3 (Ser396) mAb was purchased from Cell Signaling (Danvers, MA). The peroxidase-conjugated Affinipure goat anti-mouse IgG and peroxidase-conjugated Affinipure goat anti-rabbit IgG were purchased from Jackson Immuno Research (West Grove, PA). Alexa-Flour 488-conjugated and Alexa-Flour 594-conjugated secondary antibodies were purchased from Invitrogen (Carlsbad, CA).

Plasmids and DNA cloning

The plasmids pFLAG-nsp1, pFLAG-nsp1α and pFLAG-nsp1β contain the full-length nsp1, nsp1α, and nsp1β genes of PRRSV, respectively, fused with an N-terminal FLAG tag (Han et al., 2013; Song et al., 2010). The full sequence of LDV nsp1, EAV nsp1, SHFV nsp1, and their subunits including the N- or C-terminal FLAG tag were amplified by PCR using cDNA clones of LDV, EAV, and SHFV using primer sets listed in Table 1. The SHFV–nsp1 gene was kindly provided by Eric Snijder (Leiden University Medical Center, Leiden, Netherlands). The PCR fragments were cloned into the pXJ41 mammalian expression vector using the indicated restriction enzymes (Xiao et al., 1991). Mutant genes were generated by PCR-based site-directed mutagenesis using primers listed in

Table 2
Mutagenic oligonucleotides and their sequences.

Oligonucleotides	Primer sequence
SC246A-Fwd	5′-CTTTGAGCATGGCCGCGCCTGGCTGAAGTTGTTC-3′
SC246A-Rev	5′-GAACAACTTCAGCCAGGCGCGGCCATGCTCAAAG-3′
SH309A-Fwd	5′-ATCTTGGCTCGGGGCCATCGGTCATGCCG-3′
SH309A-Rev	5′-CGGCATGACCGATGGCCCCGAGCCAAGATC-3′
SC378A-Fwd	5′-CCCTCACTGCTGGGTTCGCTTGGTTGCAGCTATTTC-3′
SC378A-Rev	5′-GAAATAGCTGCAACCAAGCGAACCCAGCAGTGAGGG-3′
SH433A-Fwd	5′-CTAGTGATTCTTCCATCAGAGCCATTTCTCCCGTCCCTATAC-3′
SH433A-Fwd	5′-GTATAGGGACGGGAGAAATGGCTCTGATGGAAGAAT CACTAG-3′
SG164S-Fwd	5′-CAGGGAAGACTTATTTCAGTGGAAATGCCAGTTCG-3′
SG164S-Rev	5′-CGAACTGGCATTTCCACTGAAATAAGTCTTCCCTG-3′
SG164V-Fwd	5′-AGGGAAGACTTATTTCGTTGGAAATGCCAGTTCGG-3′
SG164V-Rev	5′-CCGAACTGGCATTTCCAACGAAATAAGTCTTCCCT-3′
SG165S-Fwd	5′-AGGGAAGACTTATTTCGGTAGCAATGCCAGTTCGGT TAGCT-3′
SG165S-Rev	5′-AGCTAACCGAACTGGCATTGCTACCGAAATAAGTCTTCCCT-3′
SG165V-Fwd	5′-GGAAGACTTATTTCGGTGTAAATGCCAGTTCGGTTAG-3′
SG165V-Rev	5′-CTAACCGAACTGGCATTTACACCGAAATAAGTCTTCC-3′
SG294S-Fwd	5′-GGAACGCGTTACAGTCGCCGTCGGG-3′
SG294S-Rev	5′-CCCGACGGCGACTGTAACGCGTTCC-3′
SG294V-Fwd	5′-GAACGCGTTACGTTCGCCGTCGGGG-3′
SG294V-Rev	5′-CCCCGACGGCGAACGTAACGCGTTC-3′
SY293S-Fwd	5′-CGATTTAGGATTCGGAACGCGTAGCGGTCGCCGTCG-3′
SY293S-Rev	5′-CGACGGCGACCGCTACGCGTTCCGAATCCTAAATCG-3′
SY293V-Fwd	5′-CGATTTAGGATTCGGAACGCGTGTCGGTCGCCGTCG-3′
SY293V-Rev	5′-CGACGGCGACCGACACGCGTTCCGAATCCTAAATCG-3′
SR295S-Fwd	5′-TCGGAACGCGTTACGGTAGCCGTCGGG-3′
SR295S-Rev	5′-CCCGACGGCTACCGTAACGCGTTCCGA-3′
SR295V-Fwd	5′-TCGGAACGCGTTACGGTGTCCGTCGGGG-3′
SR295V-Rev	5′-CCCCGACGGACACCGTAACGCGTTCCGA-3′

Table 1
Oligonucleotides used for cloning nsp1 genes and their sequences.

Oligonucleotides	Primer sequence
LDV-F-nsp1α-Fwd	5′-GCCGAATTCCACCATG*GATTACAAGGATGACGACGATAAG*ATGCAGTCGGGATTCG-3′
LDV-F-nsp1α-Rev	5′-GCCCTCGAGCTATCGTGCATCAGCAAAAGGACAT-3′
LDV-F-nsp1β-Fwd	5′-GCCGGATCCACCATG*GATTACAAGGATGACGACGATAAG*GCGAATGTGTGGCGTTAC-3′
LDV-F-nsp1β-Rev	5′-GCCGGTACCCTACCCATAGTATTTTCTAGTTTGGAATCTA-3′
EAV-F-nsp1-Fwd	5′-GCCGAATTCACCATG*GATTACAAGGATGACGACGATAAG*ATGGCAACCTTCTCCGC-3′
EAV-F-nsp1-Rev	5′-GCCCTCGAGCTAGCCGTAGTTGCCAGCAGGC-3′
SHFV-F-nsp1α-Fwd	5′-GCCGAATTCACCATG*GATTACAAGGATGACGACGATAAG*TTCTGTGAGTGCCC-3’
SHFV-F-nsp1α-Rev	5′-GCCCTCGAGCTATGCATGCCACTCGACATGATCTATG-3′
SHFV-F-nsp1β- Fwd	5′-GCCGAATTCACCATG*GATTACAAGGATGACGACGATAAG*GGTGTTAAGCCTGG-3′
SHFV-F-nsp1β-Rev	5′-GCCCTCGAGCTAACCGAAATAAGTCTTCCC-3′
SHFV–nsp1β-F-Rev	5′–GCCCTCGAGCTA*CTTATCGTCGTCATCCTTGTAATC*ACCGAAATAAGTCTTCCC-3′
SHFV-F-nsp1γ- Fwd	5′–GCCGAATTCACCATG*GATTACAAGGATGACGACGATAAG*GGAAATGCCAGTTCGG-3′
SHFV-F-nsp1γ-Rev	5′–GCCCTCGAGCTAGTAACGCGTTCCGAATCC-3′
SHFV-F-nsp1γ/2 P-Rev	5'-GCCCTCGAGCTAGTCTGTAGTGACTTTGG-3′

Restriction enzyme recognition sequences are underlined. The FLAG tag is italicized and underlined.

Table 3
Subcellular distribution and IFN suppression phenotypes of the individual subunits of arterivirus nsp1.

Virus	Subunits	Cellular distribution		Activity suppression			
		Cytoplasm	Nucleus	IFN	IRF3	CBP	ISRE
PRRSV	nsp1α	+++	++	+++	−	+++	++
	nsp1β	+	+++	+++	−	−	+++
LDV	nsp1α	+++	++	+++	−	+++	++
	nsp1β	+	+++	+++	−	−	+++
EAV	nsp1	+	+++	+++	−	−	++
SHFV	nsp1αβ	++	++	+++	−	−	++
	nsp1γ	+	+++	+++	−	+	++

The symbols denotes the presence (+) or absence (−) of indicated phenotypes. Staining Intensities are expressed as + (weak), ++ (medium), and +++ (strong).

Table 2. Reporter plasmids, pIFN-β-Luc and p4xIRF3-Luc were kindly provided by Stephan Ludwig (Ehrhardt et al., 2004; Institute of Molecular Medicine, Heinrich Heine Universtät, Düsseldorf, Germany), and used for luciferase assays. The p4xIRF3-Luc construct contains four copies of the IRF3-specific PRDI/III domain of the IFN-β promoter in front of the luciferase reporter gene. The plasmid pPRDII-Luc contains two copies of the NF-κB-specific PRDII binding region of the IFN-β promoter in front of the luciferase gene and was kindly provided by Stanley Perlman (University of Iowa, IA; Zhou and Perlman, 2007). The plasmid pISRE-Luc contains the IFN stimulated response element (ISRE) binding sequence and was purchased from Stratagene (La Jolla, CA). The *Renilla* luciferase plasmid pRL-TK contains the herpes simplex virus thymidine kinase (HSV-*tk*) promoter and was included to serve as an internal control in luciferase reporter assay (Promega).

DNA transfection and protein expression

DNA transfection was performed in HeLa or MARC-145 cells using Lipofectamine 2000 according to the manufacturer's instructions (Invitrogen; Carlsbad, CA). HeLa or MARC-145 cells were seeded in 6-well plates a day prior to transfection and grown to 80% confluency. A transfection mix containing DNA and Lipofectamine 2000 in OPTI-MEM® I (Invitrogen; Carlsbad, CA) was incubated at room temperature (R/T) for 20 min and added to each well. After incubation, the transfection mix was replaced with a fresh medium, and cells were incubated for 24 h to allow gene expression.

Western blot analysis

Cells were lysed in lysis buffer (20 mM Tris [pH 7.5], 150 mM NaCl, 1 mM EDTA, 1 mM EGTA, 1% Triton X-100, 1% NP-40) supplemented with a cocktail of protease inhibitors (P-8340 Sigma). Cell lysates were centrifuged and supernatants were resolved by 7.5%, 10%, or 12% SDS-PAGE, followed by transfer to Immobilon-P membrane (Millipore). After blocking with 5% skim milk powder in TBS-T (10 mM Tris–HCl [pH 8.0], 150 mM NaCl, 1% Tween 20), membranes were incubated with primary antibody dissolved in TBS-T containing 5% skim milk powder for 1 h at R/T followed by washing and incubation with horseradish peroxidase-conjugated secondary antibody for 1 h at R/T. After three washes with TBS-T, proteins were visualized using the Enhanced Chemiluminescence system (Pierce, Rockford, IL). Digital signal acquisition and analysis were conducted using GraphPad Prism 5.0 (GraphPad).

Immunofluorescence analysis (IFA)

Cells were seeded on cover slips and transfected with individual plasmids for 24 h. After washing with phosphate-buffered saline (PBS), cells were fixed with 4% paraformaldehyde for 10 min at R/T in (PBS), and then permeabilized using 0.1% Triton X-100 for 10 min at R/T. After blocking with 1% BSA in PBS for 30 min, cells were incubated with primary antibody in PBS containing 1% BSA for 2 h followed by incubation with Alexa Fluor 488- and/or Alexa Fluor 594-conjugated secondary antibody for 1 h. Nuclear staining was performed with DAPI for 3 min at R/T. After washing with PBS, coverslips were mounted onto microscope slides using Fluoromount-G mounting medium (Southern Biotech, Birmingham, AL), and examined under a fluorescence microscope (Leitz Laborlux 12). To quantify degradation of CBP and reduction of PML, the formula described previously (Han et al., 2013) were used to calculate the percentage of cells with visible reduction of CBP or PML-NB.

Luciferase reporter assay

HeLa cells were grown to a density of 5×10^4 cells/well in 12-well plates and transfected with various combination of plasmid DNA: 0.5 μg of plasmid encoding the subunit protein of nsp1, 0.5 μg of pIFN-β-Luc, pPRDII-Luc, p4xIRF3-Luc, or pISRE-Luc, and 0.05 μg of pLR-TK were co-transfected using Lipofectamine. At 24 h post-transfection, cells were stimualted with 0.5 μg of poly (I:C) for 16 h and cell lysates were prepared for luciferase assays. For pISRE-Luc, cells were incubated with 1000 units of human IFN (bioWORLD, Dublin, OH) for 16 h. Luciferase activities were measured using the Dual-Glo Luciferase assay system according to the manufacturer's instructions (Promega). Values for each sample were normalized using *Renilla* luciferase activities and the results were expressed as relative luciferase activities. All assays were repeated at least three times, and each sample was analyzed in triplicates.

VSIV-GFP bioassay

HeLa cells in 6-well plates were transfected with 2 μg of plasmids expressing individual subunit of arterivirus nsp1. At 24 h post-transfection, cells were stimulated with 1 μg of poly (I:C) by transfection and continued incubation for 12 h. Supernatant was harvested and serially diluted by 2-folds. MARC-145 cells were grown in 96-well plates and incubated for 24 h with 100 μl of each dilution of the supernatant. Cells were then infected with 100 μl of VSIV-GFP of 10^4 PFU/ml and incubated for 16 h. Cells were fixed with 4% paraformaldehyde, and GFP expression was examined under an inverted fluorescence microscopy (Nikon Eclipse TS100).

Acknowledgments

This study was supported by funding to D. Yoo from Agriculture and Food Research Initiative (AFRI) Competitive Grant no. 2013-67015-21243 of the US Department of Agriculture (USDA) National Institute of Food and Agriculture, USDA Multi-State Research Funds, and the US National Pork Board.

References

Albina, E., Carrat, C., Charley, B., 1998. Interferon-alpha response to swine arterivirus (PoAV), the porcine reproductive and respiratory syndrome virus. J. Interferon Cytokin. Res. 18, 485–490.

Allende, R., Lewis, T.L., Lu, Z., Rock, D.L., Kutish, G.F., Ali, A., Doster, A.R., Osorio, F.A., 1999. North American and European porcine reproductive and respiratory

syndrome viruses differ in non-structural protein coding regions. J. Gen. Virol. 80, 307–315.
Anderson, G.W., Rowland, R.R.R., Palmer, G.A., Even, C., Plagemann, P.G.W., 1995. Lactate dehydrogenase-elevating virus-replication persists in liver, spleen, lymph-node, and testis tissues and results in accumulation of viral-RNA in germinal-centers, concomitant with polyclonal activation of B-cells. J. Virol. 69, 5177–5185.
Baccala, R., Hoebe, K., Kono, D.H., Beutler, B., Theofilopoulos, A.N., 2007. TLR-dependent and TLR-independent pathways of type I interferon induction in systemic autoimmunity. Nat. Med. 13, 543–551.
Beura, L.K., Sarkar, S.N., Kwon, B., Subramaniam, S., Jones, C., Pattnaik, A.K., Osorio, F.A., 2010. Porcine reproductive and respiratory syndrome virus nonstructural protein 1beta modulates host innate immune response by antagonizing IRF3 activation. J. Virol. 84, 1574–1584.
Beura, L.K., Subramaniam, S., Vu, H.L., Kwon, B., Pattnaik, A.K., Osorio, F.A., 2012. Identification of amino acid residues important for anti-IFN activity of porcine reproductive and respiratory syndrome virus non-structural protein 1. Virology 433, 431–439.
Chelbi-Alix, M.K., Pelicano, L., Quignon, F., Koken, M.H., Venturini, L., Stadler, M., Pavlovic, J., Degos, L., de The, H., 1995. Induction of the PML protein by interferons in normal and APL cells. Leukemia 9, 2027–2033.
Chen, Z., Lawson, S., Sun, Z., Zhou, X., Guan, X., Christopher-Hennings, J., Nelson, E. A., Fang, Y., 2010. Identification of two auto-cleavage products of nonstructural protein 1 (nsp1) in porcine reproductive and respiratory syndrome virus infected cells: nsp1 function as interferon antagonist. Virology 398, 87–97.
Dalton, K.P., Rose, J.K., 2001. Vesicular stomatitis virus glycoprotein containing the entire green fluorescent protein on its cytoplasmic domain is incorporated efficiently into virus particles. Virology 279, 414–421.
den Boon, J.A., Snijder, E.J., Chirnside, E.D., Devries, A.A.F., Horzinek, M.C., Spaan, W.J.M., 1991. Equine arteritis virus is not a togavirus but belongs to the coronaviruslike superfamily. J. Virol. 65, 2910–2920.
Dyck, J.A., Maul, G.G., Miller Jr., W.H., Chen, J.D., Kakizuka, A., Evans, R.M., 1994. A novel macromolecular structure is a target of the promyelocyte-retinoic acid receptor oncoprotein. Cell 76, 333–343.
Ehrhardt, C., Kardinal, C., Wurzer, W.J., Wolff, T., von Eichel-Streiber, C., Pleschka, S., Planz, O., Ludwig, S., 2004. Rac1 and PAK1 are upstream of IKK-epsilon and TBK-1 in the viral activation of interferon regulatory factor-3. FEBS Lett. 567, 230–238.
Fang, Y., Snijder, E.J., 2010. The PRRSV replicase: exploring the multifunctionality of an intriguing set of nonstructural proteins. Virus Res. 154, 61–76.
Fang, Y., Treffers, E.E., Li, Y., Tas, A., Sun, Z., van der Meer, Y., de Ru, A.H., van Veelen, P.A., Atkins, J.F., Snijder, E.J., Firth, A.E., 2012. Efficient-2 frameshifting by mammalian ribosomes to synthesize an additional arterivirus protein. Proc. Natl. Acad. Sci. USA 109, E2920–E2928.
Firth, A.E., Zevenhoven-Dobbe, J.C., Wills, N.M., Go, Y.Y., Balasuriya, U.B.R., Atkins, J. F., Snijder, E.J., Posthuma, C.C., 2011. Discovery of a small arterivirus gene that overlaps the GP5 coding sequence and is important for virus production. J. Gen. Virol. 92, 1097–1106.
Godeny, E.K., de Vries, A.A., Wang, X.C., Smith, S.L., de Groot, R.J., 1998. Identification of the leader-body junctions for the viral subgenomic mRNAs and organization of the simian hemorrhagic fever virus genome: evidence for gene duplication during arterivirus evolution. J. Virol. 72, 862–867.
Han, M.Y., Du, Y.J., Song, C., Yoo, D.W., 2013. Degradation of CREB-binding protein and modulation of type I interferon induction by the zinc finger motif of the porcine reproductive and respiratory syndrome virus nsp1 alpha subunit. Virus Res. 172, 54–65.
Johnson, C.R., Griggs, T.F., Gnanandarajah, J., Murtaugh, M.P., 2011. Novel structural protein in porcine reproductive and respiratory syndrome virus encoded by an alternative ORF5 present in all arteriviruses. J. Gen. Virol. 92, 1107–1116.
Kim, H.S., Kwang, J., Yoon, I.J., Joo, H.S., Frey, M.L., 1993. Enhanced replication of porcine reproductive and respiratory syndrome (PRRS) virus in a homogeneous subpopulation of MA-104 cell line. Arch. Virol. 133, 477–483.
Kim, O., Sun, Y., Lai, F.W., Song, C., Yoo, D., 2010. Modulation of type I interferon induction by porcine reproductive and respiratory syndrome virus and degradation of CREB-binding protein by non-structural protein 1 in MARC-145 and HeLa cells. Virology 402, 315–326.
Kroese, M.V., Zevenhoven-Dobbe, J.C., Bos-de Ruijter, J.N., Peeters, B.P., Meulenberg, J.J., Cornelissen, L.A., Snijder, E.J., 2008. The nsp1alpha and nsp1 papain-like autoproteinases are essential for porcine reproductive and respiratory syndrome virus RNA synthesis. J. Gen. Virol. 89, 494–499.
Lauck, M., Hyeroba, D., Tumukunde, A., Weny, G., Lank, S.M., Chapman, C.A., O'Connor, D.H., Friedrich, T.C., Goldberg, T.L., 2011. Novel, divergent simian hemorrhagic fever viruses in a wild Ugandan red colobus monkey discovered using direct pyrosequencing. PloS One 6, e19056.
Lauck, M., Sibley, S.D., Hyeroba, D., Tumukunde, A., Weny, G., Chapman, C.A., Ting, N., Switzer, W.M., Kuhn, J.H., Friedrich, T.C., O'Connor, D.H., Goldberg, T.L., 2013. Exceptional simian hemorrhagic fever virus diversity in a wild African primate community. J. Virol. 87, 688–691.
Li, Y., Tas, A., Snijder, E.J., Fang, Y., 2012. Identification of porcine reproductive and respiratory syndrome virus ORF1a-encoded non-structural proteins in virus-infected cells. J. Gen. Virol. 93, 829–839.
Li, Y., Zhu, L., Lawson, S.R., Fang, Y., 2013. Targeted mutations in a highly conserved motif of the nsp1beta protein impair the interferon antagonizing activity of porcine reproductive and respiratory syndrome virus. J. Gen. Virol. 94, 1972–1983.
Meulenberg, J.J.M., Hulst, M.M., Demeijer, E.J., Moonen, P.L.J.M., Denbesten, A., Dekluyver, E.P., Wensvoort, G., Moormann, R.J.M., 1993. Lelystad virus, the causative agent of porcine epidemic abortion and respiratory syndrome (Pears), is related to LDV and EAV. Virology 192, 62–72.
Nedialkova, D.D., Gorbalenya, A.E., Snijder, E.J., 2010. Arterivirus nsp1 modulates the accumulation of minus-strand templates to control the relative abundance of viral mRNAs. Plos Pathog., 6.
Nelsen, C.J., Murtaugh, M.P., Faaberg, K.S., 1999. Porcine reproductive and respiratory syndrome virus comparison: divergent evolution on two continents. J. Virol. 73, 270–280.
Patel, D., Nan, Y.C., Shen, M.Y., Ritthipichai, K., Zhu, X.P., Zhang, Y.J., 2010. Porcine reproductive and respiratory syndrome virus inhibits type I interferon signaling by blocking STAT1/STAT2 nuclear translocation. J. Virol. 84, 11045–11055.
Plagemann, P.G.W., Rowland, R.R.R., Even, C., Faaberg, K.S., 1995. Lactate dehydrogenase-elevating virus – an ideal persistent virus. Springer Semin. Immunol. 17, 167–186.
Ren, J., Liu, T., Pang, L., Li, K., Garofalo, R.P., Casola, A., Bao, X., 2011. A novel mechanism for the inhibition of interferon regulatory factor-3-dependent gene expression by human respiratory syncytial virus NS1 protein. J. Gen. Virol. 92, 2153–2159.
Sadler, A.J., Williams, B.R.G., 2008. Interferon-inducible antiviral effectors. Nat. Rev. Immunol. 8, 559–568.
Samuel, C.E., 2001. Antiviral actions of interferons. Clin. Microbiol. Rev. 14, 778–809.
Sen, N., Sommer, M., Che, X., White, K., Ruyechan, W.T., Arvin, A.M., 2010. Varicella-zoster virus immediate-early protein 62 blocks interferon regulatory factor 3 (IRF3) phosphorylation at key serine residues: a novel mechanism of IRF3 inhibition among herpesviruses. J. Virol. 84, 9240–9253.
Snijder, E.J., Kikkert, M., Fang, Y., 2013. Arterivirus molecular biology and pathogenesis. J. Gen. Virol. 94, 2141–2163.
Snijder, E.J., Meulenberg, J.J.M., 1998. The molecular biology of arteriviruses. J. Gen. Virol. 79, 961–979.
Snijder, E.J., van Tol, H., Pedersen, K.W., Raamsman, M.J.B., de Vries, A.A.F., 1999. Identification of a novel structural protein of arteriviruses. J. Virol. 73, 6335–6345.
Snijder, E.J., Wassenaar, A.L., Spaan, W.J., 1992. The 5′ end of the equine arteritis virus replicase gene encodes a papainlike cysteine protease. J. Virol. 66, 7040–7048.
Song, C., Krell, P., Yoo, D., 2010. Nonstructural protein 1alpha subunit-based inhibition of NF-kappaB activation and suppression of interferon-beta production by porcine reproductive and respiratory syndrome virus. Virology 407, 268–280.
Sun, Y., Han, M.Y., Kim, C., Calvert, J.G., Yoo, D., 2012. Interplay between interferon-mediated innate immunity and porcine reproductive and respiratory syndrome virus. Viruses 4, 424–446.
Sun, Y.N., Xue, F., Guo, Y., Ma, M., Hao, N., Zhang, X.J.C., Lou, Z.Y., Li, X.M., Rao, Z.H., 2009. Crystal structure of porcine reproductive and respiratory syndrome virus leader protease nsp1 alpha. J. Virol. 83, 10931–10940.
Tijms, M.A., van der Meer, Y., Snijder, E.J., 2002. Nuclear localization of non-structural protein 1 and nucleocapsid protein of equine arteritis virus. J. Gen. Virol. 83, 795–800.
Tijms, M.A., van Dinten, L.C., Gorbalenya, A.E., Snijder, E.J., 2001. A zinc finger-containing papain-like protease couples subgenomic mRNA synthesis to genome translation in a positive-stranded RNA virus. Proc. Natl. Acad. Sci. USA 98, 1889–1894.
Van Hemert, M.J., Snijder, E.J., 2007. Nidoviruses, the Arterivirus Replicase, pp. 83–101 (Chapter 6).
Wang, R., Nan, Y.C., Yu, Y., Zhang, Y.J., 2013. Porcine reproductive and respiratory syndrome virus nsp1 beta inhibits interferon-activated JAK/STAT signal transduction by inducing karyopherin-alpha 1 degradation. J. Virol. 87, 5219–5228.
Wootton, S., Yoo, D., Rogan, D., 2000. Full-length sequence of a Canadian porcine reproductive and respiratory syndrome virus (PRRSV) isolate. Arch. Virol. 145, 2297–2323.
Xiao, J.H., Davidson, I., Matthes, H., Garnier, J.M., Chambon, P., 1991. Cloning, expression, and transcriptional properties of the human enhancer factor TEF-1. Cell 65, 551–568.
Xue, F., Sun, Y.N., Yan, L.M., Zhao, C., Chen, J., Bartlam, M., Li, X.M., Lou, Z.Y., Rao, Z.H., 2010. The crystal structure of porcine reproductive and respiratory syndrome virus nonstructural protein nsp1-beta reveals a novel metal-dependent nuclease. J. Virol. 84, 6461–6471.
Yoo, D., Song, C., Sun, Y., Du, Y., Kim, O., Liu, H.C., 2010. Modulation of host cell responses and evasion strategies for porcine reproductive and respiratory syndrome virus. Virus Res. 154, 48–60.
Zhou, H.X., Perlman, S., 2007. Mouse hepatitis virus does not induce beta interferon synthesis and does not inhibit its induction by double-stranded RNA. J. Virol. 81, 568–574.
Zhu, H., Zheng, C., Xing, J., Wang, S., Li, S., Lin, R., Mossman, K.L., 2011. Varicella-zoster virus immediate-early protein ORF61 abrogates the IRF3-mediated innate immune response through degradation of activated IRF3. J. Virol. 85, 11079–11089.
Ziebuhr, J., Snijder, E.J., Gorbalenya, A.E., 2000. Virus-encoded proteinases and proteolytic processing in the *Nidovirales*. J. Gen. Virol. 81, 853–879.